

# Lepton flavour violating Higgs and $\tau \rightarrow \mu\gamma$

Sacha Davidson <sup>\*</sup> and Gerald Grenier <sup>†</sup>

*IPNL, Université de Lyon, Université Lyon 1, CNRS/IN2P3, 4 rue E. Fermi 69622 Villeurbanne cedex, France*

## Abstract

We update phenomenological constraints on a Two Higgs Doublet Model with lepton flavour non-conserving Yukawa couplings. We review that  $\tan\beta$  is ambiguous in such “Type III” models, and define it from the  $\tau$  Yukawa coupling. The neutral scalars  $\phi$  could be searched for at hadron colliders in  $\phi \rightarrow \tau\bar{\mu}$ , and are constrained by the rare decay  $\tau \rightarrow \mu\gamma$ . The Feynman diagrams for the collider process, with Higgs production via gluon fusion, are similar to the two-loop “Barr-Zee” diagrams which contribute to  $\tau \rightarrow \mu\gamma$ . Some “tuning” is required to obtain a collider cross-section of order the Standard Model expectation for  $\sigma(gg \rightarrow h_{SM} \rightarrow \tau^+\tau^-)$ , while agreeing with the current bound from  $\tau \rightarrow \mu\gamma$ .

## 1 Introduction

The Two Higgs Doublet Model (2HDM) may be the low energy effective theory for many models of Beyond-the-Standard Model (BSM) physics at the TeV scale. Various Higgses could be the first signals of BSM physics discovered at hadron colliders. The aim of this paper is therefore to study the implications for collider searches, of precision physics bounds on a generic 2HDM with lepton flavour violating couplings. Similar analyses have previously been performed in [1, 2, 3, 4, 5, 6]. We assume that the additional Higgses are the only BSM particles with masses  $\lesssim 400$  GeV, and consider constraints on the Higgs parameters which are comparatively independent of additional New Physics at higher scales.

The 2HDM [7] (see [8] for an introduction) consists in adding a second Higgs doublet to the Standard Model. Despite being a fairly minimal extension<sup>1</sup>, it has many variants. In particular, a discrete symmetry [12] can be imposed on the Higgs plus fermion Lagrangian, to avoid tree level flavour changing neutral interactions. We focus here on “Type III” models, meaning that no discrete symmetries are present, so there is no unique definition of  $\tan\beta$ . We neglect non-renormalisable operators [13, 14] in the potential. In the absence of a discrete symmetry, the fermions can couple to both Higgs doublets with generic Yukawa matrices, which allows flavour-changing tree-level couplings of the physical Higgses. For simplicity, we make the (unrealistic) assumption that our Higgses only have *lepton* flavour violating interactions<sup>2</sup>. We are particularly interested in the Higgs– $\tau$ – $\mu$  interaction.

We emphasize that, for a generic neutral Higgs  $\phi$ , the search for  $\phi \rightarrow \tau\bar{\mu}$  at hadron colliders [16, 3, 4] should take into account the bounds on  $\tau \rightarrow \mu\gamma$  [5]. In figure 1, on the left is shown a fermion loop diagram of “Barr-Zee” type [17, 18, 19, 20, 21, 22] which contributes to  $\tau \rightarrow \mu\gamma$ . Beside it is the similar diagram for Higgs production and decay to  $\tau\bar{\mu}$  at a hadron collider. In the absence of cancellations between the different neutral Higgses in the Barr-Zee, it is clear that an upper bound on  $BR(\tau \rightarrow \mu\gamma)$  sets a bound on  $\sigma(gg \rightarrow \phi \rightarrow \tau\bar{\mu})$ .

There is a large literature on flavour changing observables in the Type III 2HDM. Various textures for the Yukawa matrices are discussed in [23] (see also references therein). Recently, the concept of Minimal Flavour Violation has been extended to multi-Higgs models [24]. See also [25] for a clear discussion of CP violation in a Type III 2HDM that has no tree-level flavour changing neutral couplings. In the Minimal Supersymmetric Standard Model (MSSM), Higgs decay to  $\tau^\pm\mu^\mp$  [26], and its relation to one loop rare  $\tau$  decays [27] have been extensively studied (see also citations of [26]). Our analysis differs from [1, 3, 5] in that we have included the Barr-Zee diagram in our calculation of  $\tau \rightarrow \mu\gamma$ . This can be relevant if the flavour-changing Higgs has  $\mathcal{O}(1)$  coupling to the top (“small  $\tan\beta$ ”). The current bound on  $BR(\tau \rightarrow \mu\gamma)$  is also slightly stronger than the

<sup>\*</sup>E-mail address: s.davidson@ipnl.in2p3.fr

<sup>†</sup>E-mail address: g.grenier@ipnl.in2p3.fr

<sup>1</sup>The Higgs sector of the Minimal Supersymmetric Standard Model [9] is a 2HDM. Larger Higgs sectors with multiple doublets and singlets [10, 11], and/or triplets, can also be considered.

<sup>2</sup>See, for instance, [15] and references thereto, for a discussion of quark flavour changing interactions in type III models.

value used by [5], who performed a more complete study of  $\tau$  decay bounds in 2005. Finally, we are attentive to the definition of  $\tan\beta$ ; we allow the scalar potential of the Higgs to take its most general renormalisable CP-conserving form, which does not allow a Lagrangian-basis-independent definition of  $\tan\beta$ . The unphysical character of  $\tan\beta$  in type III models has been treated in various ways by previous authors, which makes it difficult to compare results. We introduce a “physical” definition of  $\tan\beta$ , via the Yukawa coupling of the  $\tau$ , to facilitate comparison with “almost type II” models such as the MSSM.

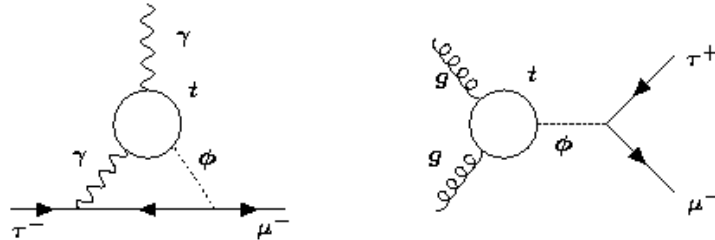


Figure 1: On the left, the “Barr-Zee” diagram which contributes to  $\tau \rightarrow \mu\gamma$ . On the right, the production/decay diagram for a neutral Higgs  $\phi$  at hadron collider.

In section 2, we introduce our “basis independent” [28, 29, 30, 31] notation for the 2HDM. We discuss electroweak precision bounds on the Higgs masses in section 3, and rapidly review bounds (for instance, on the Higgs potential) that are secondary in our analysis. Section 4 discusses the constraints from precision flavour observables, such as  $(g-2)_\mu$  and  $\tau \rightarrow \mu\gamma$ , and section 5 studies the sensitivity to the  $\phi - \tau - \mu$  Yukawa coupling of  $\phi \rightarrow \tau\bar{\mu}$  at hadron colliders, in the light of the rare decay data.

## 2 Notation

We consider a 2HDM of Type III, in the classification<sup>3</sup> used, for instance, in [28]. Contrary to “type I” and “type II” models, the type III scalar potential has no discrete symmetry that distinguishes doublets. When Yukawa couplings are included, tree-level flavour changing couplings for the neutral Higgses are possible. In an arbitrary choice of basis in doublet Higgs space, the potential can be written [33]

$$\begin{aligned} \mathcal{V} = & m_{11}^2 \Phi_1^\dagger \Phi_1 + m_{22}^2 \Phi_2^\dagger \Phi_2 - [m_{12}^2 \Phi_1^\dagger \Phi_2 + \text{h.c.}] \\ & + \frac{1}{2} \lambda_1 (\Phi_1^\dagger \Phi_1)^2 + \frac{1}{2} \lambda_2 (\Phi_2^\dagger \Phi_2)^2 + \lambda_3 (\Phi_1^\dagger \Phi_1) (\Phi_2^\dagger \Phi_2) + \lambda_4 (\Phi_1^\dagger \Phi_2) (\Phi_2^\dagger \Phi_1) \\ & + \left\{ \frac{1}{2} \lambda_5 (\Phi_1^\dagger \Phi_2)^2 + [\lambda_6 (\Phi_1^\dagger \Phi_1) + \lambda_7 (\Phi_2^\dagger \Phi_2)] \Phi_1^\dagger \Phi_2 + \text{h.c.} \right\}, \end{aligned} \quad (1)$$

where  $m_{11}^2$ ,  $m_{22}^2$ , and  $\lambda_1, \dots, \lambda_4$  are real parameters. In general,  $m_{12}^2$ ,  $\lambda_5$ ,  $\lambda_6$  and  $\lambda_7$  are complex, but we neglect CP violation in this paper for simplicity, and take them  $\in \mathbb{R}$ . A clear discussion of CP violation can be found in [34, 30]. A translation dictionary to the form of potential used, for instance, in [8], can be found in [33].

The scalar fields will develop non-zero vacuum expectation values (vevs) if the mass matrix  $m_{ij}^2$  has at least one negative eigenvalue. Then, the scalar field vacuum expectations values are of the form

$$\langle \Phi_1 \rangle = \frac{1}{\sqrt{2}} \begin{pmatrix} 0 \\ v_1 \end{pmatrix}, \quad \langle \Phi_2 \rangle = \frac{1}{\sqrt{2}} \begin{pmatrix} 0 \\ v_2 \end{pmatrix}, \quad (2)$$

where  $v_1$  and  $v_2$  are real and non-negative, and

$$v^2 \equiv v_1^2 + v_2^2 = \frac{4m_W^2}{g^2} = (246 \text{ GeV})^2 = \frac{1}{\sqrt{2}G_F} \quad \tan\beta \equiv \frac{v_2}{v_1} \quad (3)$$

<sup>3</sup>This definition differs from the classification given in [32], where there are 4 types of 2HDM, all of which avoid tree level flavour changing neutral currents.

The scalar potential of the type III 2HDM, with real couplings, has three parameters in  $m_{ij}^2$ , four in  $\lambda_{1..4}$  and three in  $\lambda_{5..7}$ . One of these parameters can be set to zero by a basis choice (for instance  $m_{12}^2 = 0$ ), leaving nine independent parameters. The minimisation conditions give  $v$ , which is measured, so 8 inputs are required. Ideally, one would like to express these parameters in terms of observables, such as masses and 3 or 4 point functions. This would avoid confusion stemming from the arbitrary basis choice in Higgs space, and clarifies the measure on parameter space to use in numerical scans.

However, to study the current bounds on “light” Higgses, we only need their masses and couplings to SM particles (controlled by  $(\beta - \alpha)$  — see the discussion after eqn (5)). So we do not need a complete parametrisation in terms of observables; we relate constraints on the scalar potential to the masses in the basis independent notation of [28], and otherwise our parameters are  $m_h^2, m_H^2, m_A^2, m_{H+}^2, \sin(\beta - \alpha)$  and the flavour changing Yukawa coupling that controls  $p\bar{p} \rightarrow \phi \rightarrow \tau\bar{\mu}$  and  $\tau \rightarrow \mu\gamma$ .

## 2.1 Basis choice in Higgs space and $\tan \beta_\tau$

It is always possible to choose a basis in the Higgs space, such that only one doublet acquires a vev [34]. This is known as the “Higgs basis”, defined such that  $\langle H_1 \rangle \neq 0$ , and  $\langle H_2 \rangle = 0$ , and in this basis all the potential parameters are written in upper case:

$$\begin{aligned} \mathcal{V} = & M_{11}^2 H_1^\dagger H_1 + M_{22}^2 H_2^\dagger H_2 - [M_{12}^2 H_1^\dagger H_2 + \text{h.c.}] \quad (\text{in Higgs basis}) \\ & + \frac{1}{2} \Lambda_1 (H_1^\dagger H_1)^2 + \frac{1}{2} \Lambda_2 (H_2^\dagger H_2)^2 + \Lambda_3 (H_1^\dagger H_1)(H_2^\dagger H_2) + \Lambda_4 (H_1^\dagger H_2)(H_2^\dagger H_1) \\ & + \left\{ \frac{1}{2} \Lambda_5 (H_1^\dagger H_2)^2 + [\Lambda_6 (H_1^\dagger H_1) + \Lambda_7 (H_2^\dagger H_2)] H_1^\dagger H_2 + \text{h.c.} \right\}, \end{aligned} \quad (4)$$

This follows the notation of [28].

In the Higgs basis, the angle  $\alpha_{HB}$  rotates to the mass basis of the CP even Higgses  $h, H$ :

$$\begin{aligned} h &= -(\sqrt{2} \operatorname{Re} H_1^0 - v) \sin \alpha_{HB} + (\sqrt{2} \operatorname{Re} H_2^0) \cos \alpha_{HB}, \\ H &= (\sqrt{2} \operatorname{Re} H_1^0 - v) \cos \alpha_{HB} + (\sqrt{2} \operatorname{Re} H_2^0) \sin \alpha_{HB}. \end{aligned} \quad (5)$$

In a 2HDM of type I or II, there is also a choice of basis where the discrete symmetry  $\Phi_i \leftrightarrow \Phi_i$ , or  $\Phi_j \leftrightarrow -\Phi_j$  is manifest. Usually, the lagrangian is written in the basis where this symmetry is manifest<sup>4</sup>, the angle  $\beta$  is defined between this “symmetry eigenbasis” and the Higgs basis, and the angle  $\alpha$  rotates between the symmetry basis and the CP-even mass basis. In which case

$$\alpha_{HB} = \beta - \alpha \quad (6)$$

and we shall write it as such in this paper. Then the Higgs- $W^+W^-$  couplings are  $igm_W C_{\phi WW} g^{\mu\nu}$  with

$$C_{hWW} = s_{\beta-\alpha}, \quad C_{HWW} = c_{\beta-\alpha}, \quad C_{AWW} = 0 \quad (7)$$

where

$$s_{\beta-\alpha} \equiv \sin(\beta - \alpha), \quad c_{\beta-\alpha} \equiv \cos(\beta - \alpha). \quad (8)$$

The trilinear couplings between a neutral Higgs and a pair of charged Higgses are  $-ivC_{\phi H+H-}$ , with [33]

$$C_{hH+H-} = \Lambda_3 s_{\beta-\alpha} - \Lambda_7 c_{\beta-\alpha}, \quad C_{HH+H-} = \Lambda_3 c_{\beta-\alpha} + \Lambda_7 s_{\beta-\alpha}, \quad C_{AH+H-} = 0 \quad (9)$$

In a type III model, there is no “symmetry basis”, so  $\tan \beta$  can not be defined from the scalar potential. To obtain a type III potential, it is not sufficient to write down a Lagrangian with  $\lambda_6, \lambda_7 \neq 0$ ; one must also check that it is not a type II or type I model, in a basis rotated with respect to the symmetry basis. For this there are basis independent “invariants”, discussed for instance in [28], which vanish in the presence of symmetries.

In phenomenological calculations,  $\tan \beta$  usually appears in Yukawa interactions, where it parametrises the relative size of the Yukawa couplings and the fermion masses. Whether it can be defined from the scalar potential of the Higgses is secondary. Various “definitions” of  $\tan \beta$ , involving fermion masses in the Higgs basis, can be envisaged [35, 28, 36, 37]. To maintain the intuition of  $\tan \beta$  as the relative size of the  $\tau$  Yukawa coupling

<sup>4</sup>For a discussion of Lagrangian basis dependence in the 2HDM, and a formalism that is “basis independent”, see, *e.g.* [28, 29, 30].

and  $\sqrt{2}m_\tau/v$ , we define  $H_\tau$  to be the Higgs that couples to the  $\tau$ , and  $\beta_\tau$  as the angle in Higgs doublet space between  $H_1$  (the vev) and  $H_\tau$ :

$$\begin{aligned} H_u &= \tilde{H}_1 \sin \beta_\tau + \tilde{H}_2 \cos \beta_\tau \\ H_\tau &= H_1 \cos \beta_\tau - H_2 \sin \beta_\tau \end{aligned} \quad (10)$$

We choose the  $\tau$  Yukawa, because we are interested in  $\tau$  flavour violation. This reduces to the usual definition in a Type II (SUSY) model, where  $\tilde{H} = i\sigma_2 H^*$ .

Finally, notice that we pursue a “bottom-up” approach, where we treat  $\tan \beta_\tau$  as a physical parameter, and calculate processes which are finite. This allows us to neglect issues related to the renormalisation of  $\tan \beta_\tau$  [35, 38, 39], such as its numerical stability, and additional factors of  $\tan \beta_\tau$  that may appear.

## 2.2 The leptonic Yukawa couplings

In the Higgs basis for the Higgses, and the mass eigenstate basis for the  $\{u_R, d_R, e_R, d_L, e_L\}$ , the Yukawa interactions of a type III 2HDM can be written

$$\begin{aligned} -\mathcal{L}_Y &= \sqrt{2} \left( \overline{q_{Lj}} \tilde{H}_1 \frac{K_{ij}^* m_i^U}{v} u_{Ri} + \overline{q_{Li}} H_1 \frac{m_i^D}{v} d_{Ri} + \overline{\ell_{Li}} H_1 \frac{m_i^E}{v} e_{Ri} \right) \\ &\quad + \overline{q_{Li}} \tilde{H}_2 [\rho^U]_{ij} u_{Rj} + \overline{q_{Li}} H_2 [\rho^D]_{ij} d_{Rj} + \overline{\ell_{Li}} H_2 [\rho^E]_{ij} e_{Rj} + \text{h.c.}, \end{aligned} \quad (11)$$

where  $K$  is the CKM matrix,  $\tilde{\ell} H_1 = \bar{\nu} H_1^+ + \bar{e} H_1^0$ ,  $\tilde{H}_i = i\sigma_2 H_i^*$ , and the generation indices are written explicitly. We are principally interested in the leptons, so we drop the superscript of  $\rho^E \rightarrow \rho$ .

If the neutral CP-even Higgses are defined to be  $h$  and  $H$ , with  $m_h \leq m_H$ , if  $A$  is the CP-odd Higgs, and if flavour violating neutral couplings are allowed in the lepton sector only, this gives the following Yukawa couplings of leptons in the Higgs mass basis

$$\begin{aligned} -\mathcal{L}_Y^{\text{leptons}} &= \bar{e}_i \left[ \frac{m_i}{v} \delta_{ij} s_{\beta-\alpha} + \frac{1}{\sqrt{2}} ([\rho]_{ij} P_R + [\rho^\dagger]_{ij} P_L) c_{\beta-\alpha} \right] e_j h \\ &\quad + \bar{e}_i \left[ \frac{m_i}{v} \delta_{ij} c_{\beta-\alpha} - \frac{1}{\sqrt{2}} ([\rho]_{ij} P_R + [\rho^\dagger]_{ij} P_L) s_{\beta-\alpha} \right] e_i H \\ &\quad + \frac{i}{\sqrt{2}} \bar{e}_i ([\rho]_{ij} P_R - [\rho^\dagger]_{ij} P_L) e A \\ &\quad + \left\{ \bar{u}_i [K \rho^D]_{ij} P_R - [\rho^{U\dagger}]_{ij} P_L \right\} d H^+ + \bar{\nu}_i [U^\dagger \rho]_{ij} P_R e H^+ + \text{h.c.} \end{aligned} \quad (12)$$

where we included the charged Higgs interactions with the quarks.  $U$  is the PMNS matrix, which we henceforth drop, assuming that the neutrinos are in the “flavour” basis. For the quarks with flavour diagonal Yukawa couplings the Lagrangian can be obtained by taking  $[\rho]$  diagonal, and substituting  $\{\rho^E, e\} \rightarrow \{\rho^D, d\}$  for down quarks, and  $\{\rho^E, e\} \rightarrow \{\rho^U, u\}$  for the ups.

From eqn (12), The neutral Higgs couplings to fermions are :

$$\begin{aligned} g_{h,ff'} &= \frac{gm_f}{2m_W} s_{\beta-\alpha} \delta_{f,f'} + \frac{\rho_{ff'}}{\sqrt{2}} c_{\beta-\alpha} \\ g_{H,ff'} &= \frac{gm_f}{2m_W} c_{\beta-\alpha} \delta_{f,f'} - \frac{\rho_{ff'}}{\sqrt{2}} s_{\beta-\alpha} \\ g_{A,ff'} &= i \frac{\rho_{ff'}}{\sqrt{2}} \quad , \end{aligned} \quad (13)$$

where  $g_{A,ff'}$  appears in the Feynman rule with a  $\gamma_5$ . For simplicity, we will take  $[\rho^E]$  hermitian, and normalise it

$$[\rho]_{ij} = -\tilde{\kappa}_{ij} \sqrt{\frac{2m_i m_j}{v^2}} = -\kappa_{ij} \tan \beta_\tau \sqrt{\frac{2m_i m_j}{v^2}} \quad (14)$$

It is tempting to expect  $|\tilde{\kappa}_{ij}| \sim 1$  [40]. However, recall the definition of  $\beta_\tau$  from the end of section 2.1: in the Higgs basis for the scalar doublets, and the mass eigenstate basis of the charged leptons, the  $\tau$  Yukawa coupling is

$$\overline{\ell_L} \left[ \frac{\sqrt{2}m_\tau}{v} H_1 + \rho_{\tau\tau} H_2 \right] \tau_R + \text{h.c.} \equiv y_\tau \overline{\ell_L} [\cos \beta_\tau H_1 - \sin \beta_\tau H_2] \tau_R + \text{h.c.} \quad (15)$$

This gives  $\tilde{\kappa}_{\tau\tau} = \tan \beta_\tau$  so we factor this out and “expect” that  $\kappa_{ij} \sim 1$ . Recall that  $\alpha_{HB} = (\beta - \alpha)$  is a physical mixing angle defined from the scalar potential, not the difference of two angles. In particular, the  $\beta$  in  $(\beta - \alpha)$  is unrelated to  $\tan \beta_\tau$ .

We are interested in  $\tau - \mu$  lepton flavour violation, so we allow an arbitrary  $\kappa_{\tau\mu}$ , and assume that  $\kappa_{\tau e} \sim \kappa_{e\mu} \sim 0$ . To perform a general analysis, we should treat the  $\rho_{\phi tt}$  and  $\rho_{\phi bb}$  as free parameters, because the angle  $\beta_f$ , defined for a fermion  $f$  in analogy with eqn (15), could be different for each  $f$ . However, we attribute Type II values:

$$[\rho^D]_{ij} = -\sqrt{2} \tan \beta_\tau \frac{m_i^D}{v} \delta_{ij} \quad , \quad [\rho^U]_{ij} = \sqrt{2} \cot \beta_\tau \frac{K^\dagger m_i^U}{v} \delta_{ij} \quad , \quad [\rho^E]_{\tau\tau} = -\sqrt{2} \tan \beta_\tau \frac{m_\tau}{v} \quad . \quad (16)$$

to all elements of the  $[\rho]$  matrices (except  $\rho_{\tau\mu}$ ), because this parametrisation is adequately representative of the cases we are interested in (see the discussion at the end of section 4.4). The expressions of eqn (16) apply in the mass eigenstate bases of  $\{d_L, e_L, d_R, u_R, e_R\}$ . For a Type III model which has Type II couplings plus small corrections (as can arise in Supersymmetry[41, 26]), the  $\rho$ -coupling to the top quark is suppressed at large  $\tan \beta$ . If in addition, either  $s_{\beta-\alpha}$  or  $c_{\beta-\alpha}$  is small, eqn (13) shows that the CP-even Higgs with larger flavour-violating coupling, will be weakly coupled to the top. This suppresses both the diagrams in figure 1.

There are many notations for Type III Yukawa couplings. Our  $\kappa$  bears no relation to the one in [28], but is proportional to the  $\kappa$  of [5](KOT), who define:

$$\frac{m_\tau}{v \cos^2 \beta} (\kappa_{\tau\mu}^L + \kappa_{\mu\tau}^R) \Big|_{KOT} = -\kappa_{\tau\mu} \tan \beta_\tau \sqrt{\frac{m_\tau m_\mu}{v^2}} \Big|_{this \ paper} \quad (17)$$

The additional power of  $1/\cos \beta$  in the LFV Lagrangian of KOT causes their LFV rates to scale as  $\tan^6 \beta$ , rather than  $\tan^4 \beta_\tau$  as we find. Such differences must be taken into account in comparing plots. To ensure that our results are as “physical” as possible, we plot bounds on  $(\kappa_{\tau\mu} \tan \beta_\tau)$ , as a function of Higgs masses,  $s_{\beta-\alpha}$  from eqns (6,8) and  $\tan \beta_\tau$  defined from eqn (15).

### 3 Higgs mass bounds

In this section, we list bounds on the parameters of the scalar potential of eqn (1). These bounds were recently presented in basis-independent notation, allowing for CP-violation, in [42], where references to the earlier literature can also be found. The bounds can be divided into two classes: firstly, those which apply directly to the physical masses and coupling constants. These arise from precision electroweak analyses (the  $T$  parameter), and are the most stringent. Secondly, there are bounds on the  $\lambda_i$  couplings, which follow from imposing that  $WW \rightarrow WW$  is unitary at tree level, and from various considerations about the Higgs potential (positive, perturbative...). These must be re-expressed as bounds on the masses. In our “phenomenological” approach, where we allow arbitrary New Physics at the TeV scale, these bounds are less important. We review them briefly anyway.

#### 3.1 Bounds on the potential

We are interested in bounds on the various Higgs masses. In the Higgs basis, these are related to potential parameters as [28] :

$$m_{H+}^2 = M_{22}^2 + \frac{v^2}{2} \Lambda_3 \quad (18)$$

$$m_A^2 - m_{H+}^2 = -\frac{v^2}{2} (\Lambda_5 - \Lambda_4) \quad (19)$$

$$m_H^2 + m_h^2 - m_A^2 = +v^2 (\Lambda_1 + \Lambda_5) \quad (20)$$

$$(m_H^2 - m_h^2)^2 = [m_A^2 + (\Lambda_5 - \Lambda_1)v^2]^2 + 4\Lambda_6^2 v^4 \quad (21)$$

$$\sin[2(\beta - \alpha)] = -\frac{2\Lambda_6 v^2}{m_H^2 - m_h^2} \quad (22)$$

The  $H^\pm$  mass can be raised high enough to respect  $b$  physics bounds (see section 3.2) by increasing  $M_{22}^2$  (the decoupling limit [33]). To keep  $H, A$  light in this limit requires large  $\Lambda$ s.

### 3.1.1 vacuum stability/bounded from below (lower bound on $m_\phi$ )

The requirement that the electroweak vacuum be stable, or that the Higgs potential be bounded from below, gives a lower bound on  $m_h$ . See [43, 44] for a review. The constraint is imposed at tree level; one can also include radiative corrections and check that potential remains bounded from below.

Necessary and sufficient conditions to obtain  $V(v_i \rightarrow \infty) > 0$ , in the softly broken 2HDM type II (in the basis where  $\lambda_6 = \lambda_7 = 0$ ) were given in [33]. A basis-independent analytic discussion of Type II and Type III can be found in [45]. However, the Type III bounds do not give simple analytic formulae; a more extensive and numerical analysis was performed by [46, 47], who find a lower bound

$$m_H > 121 \text{ GeV} . \quad (23)$$

### 3.1.2 triviality/perturbativity (upper bound on $m_\phi$ )

An upper bound on the Higgs masses (which are  $\propto \lambda_i$ ) can be obtained from requiring that the  $\lambda_i$  couplings remain perturbative at higher energy scales. One can, for instance, impose that the Landau Pole of the Higgs couplings be at some sufficiently high scale. The analysis of [46] finds no upper bound on  $m_{H,A,H^\pm}^2$  for a softly broken Type II, or Type III.

### 3.1.3 Unitarity

In the spontaneously broken electroweak theory, there are delicate cancellations in the tree-level amplitude for longitudinal  $W$  scattering, between diagrams with Higgs or gauge boson exchange. In addition, at scales  $\sqrt{s} \gg$  the Higgs masses, the various scattering amplitudes are proportional to combinations of the  $\lambda_i$  couplings. S-matrix unitarity gives an upper bound on the S-matrix elements. If the tree level calculation is a good approximation to the full S-matrix, then this bound translates to bounds on the Higgs masses. These constraints are most interesting for the  $J = 0$  partial wave. This is discussed for the Standard Model in [8, 48], and in [49, 50] for the 2HDM (see also the appendix of [42]).

S-matrix unitarity implies that  $1 = SS^\dagger = (1 + iT)(1 - iT^\dagger)$ . Writing the S-matrix between states labelled by angular momentum  $J, K, \dots$  and all other quantum numbers called  $j, k, \dots$ , this gives

$$-2\text{Im}\{\langle j, J|T|k, K \rangle\} = \langle j, J|TT^\dagger|k, K \rangle \quad (24)$$

which, applied to the  $J = 0$  component of an amplitude:

$$a_0 = \frac{1}{16\pi s} \int_{-s}^0 dt \mathcal{A}$$

implies  $2|\text{Im}\{a_0\}| > |a_0|^2$ .

There are two limits in which unitarity bounds are usually calculated. The standard calculation assumes  $m_W^2 \ll m_\phi^2 \ll s$ , neglects all masses ( $\phi$  is an arbitrary Higgs), describes the longitudinal gauge bosons as Higgses via the Equivalence Theorem (see [51] for a pedagogical discussion), and obtains bounds on linear combinations of the  $\Lambda_i$  (see [50, 42] for a basis-independent calculation in the 2HDM). Notice that in the strict Type II model ( $m_{12}^2 = 0$  in the basis where  $\lambda_6 = \lambda_7 = 0$ ), these bounds are quite sensitive to  $\tan \beta$  [49]; this may be related to the appearance of a massless Higgs, in the limit where one of the vevs  $v_i \rightarrow 0$ . This is no longer the case when  $m_{12}^2 \neq 0$  is allowed [52, 50].

Here, we are more interested in the limit  $m_W^2 \ll s \ll m_\phi^2$ , where  $\phi$  is some of the Higgses. That is, we allow arbitrary New Physics at the TeV scale to preserve S-matrix unitarity in the  $m_W^2 \ll m_h^2 \ll s$  limit, but we would like to know the bounds arising on mass splitting among the Higgses, at  $\sqrt{s} < \text{TeV}$ , when some Higgses are heavier than  $\sqrt{s}$ , and some are lighter.

The gauge contribution to longitudinal  $W$  scattering (no Higgses exchanged in  $s$  or  $t$  channel), is [48]

$$\mathcal{A}(W_L W_L \rightarrow W_L W_L) = \frac{ig^2}{4m_W^2}(s+t) + \dots \quad \text{no Higgs.} \quad (25)$$

Requiring  $a_0 < 1$  implies the scale of Higgs masses should be  $\lesssim \text{TeV}$ . In the case where some Higgses are light, for instance  $m_h < s$ , including them in the amplitude reduces the coefficient of  $s+t$ , and raises the upper bound on the masses of the remaining Higgses. We conclude that unitarity constraints do not give us relevant bounds on the mass differences among the Higgses.

### 3.1.4 Electroweak precision tests

New physics that couples weakly to Standard Model fermions, but has electroweak gauge interactions, can be constrained by the measured values of the “oblique parameters” [53, 54]. If the vacuum polarisation tensor between gauge bosons  $i$  and  $j$  is defined as

$$\Pi_{ij}^{\mu\nu}(q) = g^{\mu\nu} A_{ij}(q^2) + q^\mu q^\nu B_{ij}(q^2) \quad (26)$$

then the parameters  $S$  and  $T$  can be defined as [11]

$$\bar{S} = \frac{\alpha}{4s_W^2 c_W^2} S = \frac{A_{ZZ}(m_Z^2) - A_{ZZ}(0)}{m_Z^2} + \frac{\partial A_{\gamma\gamma}}{\partial q^2} \Big|_{q^2=0} + \frac{c_W^2 - s_W^2}{s_W c_W} \frac{\partial A_{\gamma Z}}{\partial q^2} \Big|_{q^2=0} \quad (27)$$

$$\bar{T} = \alpha T = \frac{A_{WW}(0)}{m_W^2} - \frac{A_{ZZ}(0)}{m_Z^2} \quad (28)$$

where  $s_W = \sin \theta_W$ . The Standard Model contributions to these parameters, including that of the SM Higgs, are assumed to be subtracted out. The contributions to  $S, T$ , and  $U$ , (as well as  $V, W$  and  $X$ ), due to an arbitrary number of Higgs doublets and singlets have recently been calculated in [11].  $S, T$  and  $U$  were calculated in the CP violating 2HDM in [42]. We use here the formulae of [11], which verify the previous calculations of [55, 56] for the 2HDM.

As discussed in [42], the 2HDM contributions to  $S$  and  $U$  tend to be small enough, but the contribution to  $T$  can exceed the value allowed for New Physics ( $-0.15 < T < 0.20$  at one  $\sigma$  [53]). We impose the bound  $-0.05 < T - S < 0.10$  at one  $\sigma$  [53]. The calculation of  $T$  in multi-Higgs models is presented in detail in the first paper of [11]. They give

$$\begin{aligned} T = & \frac{1}{16\pi s_W^2 m_W^2} \{ F(m_A^2, m_{H+}^2) + c_{\beta-\alpha}^2 [F(m_{H+}^2, m_h^2) - F(m_A^2, m_h^2)] \\ & + s_{\beta-\alpha}^2 [F(m_{H+}^2, m_H^2) - F(m_A^2, m_H^2)] \\ & - 3c_{\beta-\alpha}^2 [F(m_Z^2, m_h^2) - F(m_W^2, m_h^2) + F(m_W^2, m_H^2) - F(m_Z^2, m_H^2)] \} \end{aligned} \quad (29)$$

where

$$F(x, y) = \frac{x+y}{2} - \frac{xy}{x-y} \ln \frac{x}{y} \quad (30)$$

is a positive function, that vanishes for degenerate masses. So as masses in the loop split, the contribution increases.

It is well known, and clear by inspection, that  $T$  becomes small in various limits, such as  $m_A \rightarrow m_{H+}$ , or  $m_H \rightarrow m_{H+}$  when  $s_{\beta-\alpha} \rightarrow 1$ . When studying  $h$  and  $H$  production and decay at colliders, we will assure the precision constraint by imposing  $m_A \simeq m_{H+} \pm 10$  GeV. For  $h$  production, we do not consider the parameters  $m_H \rightarrow m_{H+}$  and  $s_{\beta-\alpha} \rightarrow 1$ , because  $\sigma(gg \rightarrow h \rightarrow \tau^\pm \mu^\mp) \propto s_{\beta-\alpha}^2 c_{\beta-\alpha}^2$ . The collider cross-section for the pseudo-scalar  $A$  is not suppressed by  $s_{\beta-\alpha}$  or  $c_{\beta-\alpha}$ , so when we study  $\sigma(gg \rightarrow A \rightarrow \tau^\pm \mu^\mp)$ , we can ensure the precision constraint by requiring  $m_H \simeq m_{H+} \pm 10$  GeV and  $s_{\beta-\alpha} \rightarrow 1$ . For  $m_A > 100$  GeV,  $T - S$  is within the  $1 \sigma$  allowed range for  $\pi/3 < \beta - \alpha \leq \pi/2$ .

## 3.2 Flavour physics bounds

The charged Higgs  $H^+$  necessarily has tree level flavour-changing couplings, like the  $W^+$ . Its mass is therefore constrained by various flavour-changing observables, such as  $b \rightarrow s\gamma$  and  $B^+ \rightarrow \tau^+ \nu$ . The various bounds have been discussed in [57], who find  $m_{H+} > 250 \text{ GeV}$  for  $2 < \tan \beta < 20$ , and  $m_{H+} > 300 \text{ GeV}$  for  $\tan \beta < 50$ . This limit is lower than that of Misiak *et al.* from  $b \rightarrow s\gamma$  [58], which is  $m_{H+} > 300$  GeV (at  $2\sigma$ ), because of differences in the procedure of extraction of the bound.

The charged Higgs contributes at tree level to the decay of pseudoscalar mesons  $M$ . Since the SM  $W$ -mediated amplitude is helicity suppressed, the additional suppression of the Higgs amplitude is only a factor  $\sim (m_M/m_{H+})^2$  [59]. Charged meson decays, such as  $B^+ \rightarrow \tau^+ \nu$ , therefore constrain the mass and couplings of  $H^+$  in type I and type II models. In addition, they can constrain the flavour-violating couplings of type III models. It was shown in [60], that a precise determination of  $R_K = \Gamma(K^- \rightarrow e\bar{\nu})/\Gamma(K^- \rightarrow \mu\bar{\nu})$ , by the NA62 experiment, could be a sensitive test of the  $\rho_{\tau\mu}$  coupling.

### 3.3 Summary

We retain two constraints from this section:  $m_{H^+} \gtrsim 300$  GeV from B physics (as discussed in section 3.2), and the  $T$  parameter will be small enough in two cases: either  $m_A \simeq m_{H^+}$  (we take numerically  $m_A = m_{H^+} \pm 10$  GeV, or  $m_H \simeq m_{H^+}$ , with  $\beta - \alpha \gtrsim \pi/3$  to ensure  $c_{\beta-\alpha} \rightarrow 0$ ).

## 4 Constraints on flavour changing Yukawa couplings to leptons

In this section, we include the lepton flavour-changing Yukawa couplings of the Higgses, see eqn (12). We consider mass ranges for the neutral Higgs which are consistent with the constraints discussed in the previous sections, and study the sensitivity of  $(g-2)_\mu$ ,  $\tau \rightarrow \mu\gamma$  and  $\tau \rightarrow \eta\mu$  to the flavour-changing coupling  $\rho_{\tau\mu}$ , introduced in eqn (14).

A systematic study of bounds on a 2HDM (Type II), with lepton flavour violating Yukawa couplings, has been performed in [5]. They impose constraints on  $\rho_{\tau\mu}$  arising from tree and one-loop contributions to rare decays, then study the  $\phi \rightarrow \tau\bar{\mu}$  decay rate at colliders. As this is a Type II analysis,  $\tan\beta$  appears in the formulae. In the context of supersymmetric models [27], it was shown in [68] that the bounds from one and two loop contributions to  $\tau \rightarrow \ell\gamma$  are more stringent than those from  $\tau \rightarrow 3\ell$  (except if the Higgses are very degenerate).

The anomalous magnetic moment of the muon can also be sensitive to a 2HDM with flavour-violating Yukawa couplings [3, 4, 69, 71]. For  $\rho_{\tau\mu} \sim 10\sqrt{m_\tau m_\mu}/v$ , the 2HDM can fit the current discrepancy in  $(g-2)_\mu$ . However, as we will show, the constraint from  $\tau \rightarrow \mu\gamma$  precludes the explanation of the  $(g-2)_\mu$  discrepancy, for large areas of parameter space.

### 4.1 The decay $\tau \rightarrow \eta\mu$

It was shown in [5], that  $\tau \rightarrow \eta\mu$  gives a relevant constraint on  $\kappa_{\tau\mu}$  for light pseudoscalars  $A$ . We briefly review here their discussion, using the updated bound [61]  $BR(\tau \rightarrow \eta\mu) < 6.5 \times 10^{-8}$ .

The branching ratio is

$$\frac{BR(\tau \rightarrow \eta\mu)}{BR(\tau \rightarrow \mu\nu\bar{\nu})} \simeq 54\pi^2 \left(\frac{m_\eta}{m_A}\right)^4 \frac{f_\eta^2}{m_\tau^2} |\kappa_{\tau\mu}|^2 \tan^2 \beta_\tau \frac{m_\mu(m_u \cot \beta_\tau + (m_d - 2m_s) \tan \beta_\tau)^2}{(m_u + m_d + 4m_s)^2} \quad (31)$$

where  $BR(\tau \rightarrow \mu\nu\bar{\nu}) = .17$ , and  $f_\eta \simeq f_\pi$  from [62]. The current experimental upper bound gives

$$|\kappa_{\tau\mu}| \tan^2 \beta_\tau < 70 \left(\frac{m_A}{100 \text{ GeV}}\right)^2 \quad (32)$$

where we approximate the final fraction of (31) as  $\tan^2 \beta_\tau/4$ . The bound (32) agrees with the result given in [5]. This is comparable to the bound from  $\tau \rightarrow \mu\gamma$  (see figure 3); we see that a light  $A$  is allowed for small  $\tan \beta_\tau$ .

### 4.2 The dipole effective operator

Bounds on a large class of effective operators that change  $\tau - \mu$  flavour are presented in [62]. Several bounds arise from the dipole operators, which can be included in an effective Lagrangian as [63]

$$\frac{C^{ij}}{\Lambda_{NP}^2} \langle H \rangle \bar{e}_i \sigma^{\alpha\beta} P_R e_j F_{\alpha\beta} + h.c. \quad (33)$$

where  $i, j$  are the flavours of the external leptons. The chirality flipping operator must contain an odd number of Yukawa couplings, including  $\rho_{\tau\mu}$  and a flavour diagonal Yukawa coupling of the external Higgs vev. The model-dependent coefficient  $C^{ij}/\Lambda_{NP}^2$ , can be related to a New Physics contribution  $\delta a_\mu$  to the anomalous magnetic moment of the muon, and to the  $A_{L,R}$  factors that appear in  $\tau \rightarrow \mu\gamma$  [63]:

$$\frac{e\delta a_\mu}{4m_\mu} = \frac{\text{Re}\{C^{\mu\mu}\}}{\Lambda_{NP}^2} \frac{v}{\sqrt{2}} \quad \frac{em_\tau A_R^{\tau\mu}}{2} = \frac{C^{\tau\mu}}{\Lambda_{NP}^2} \frac{v}{\sqrt{2}} \quad \frac{em_\tau A_L^{\tau\mu}}{2} = \frac{C^{\mu\tau*}}{\Lambda_{NP}^2} \frac{v}{\sqrt{2}} \quad (34)$$

The  $A_{L,R}$  appear in the  $\tau \rightarrow \mu\gamma$  branching ratio as:

$$\frac{\Gamma(\tau \rightarrow \mu\gamma)}{\Gamma(\tau \rightarrow \mu\nu\bar{\nu})} = \frac{48\pi^3\alpha}{G_F^2} (A_L^2 + A_R^2) < \frac{4.4 \times 10^{-8}}{.17} \quad (35)$$



where we used the current  $\tau \rightarrow \mu\gamma$  bound [64] (very similar to the  $BR < 4.5 \times 10^{-8}$  of [65]) to obtain  $|A_L| = |A_R| \lesssim 10^{-4}G_F$ .

The current experimental and theoretical determinations of  $(g-2)_\mu$  are [53]:

$$\frac{(g-2)_\mu}{2} = a_\mu = \begin{cases} 11659208.0(5.4)(3.3) \times 10^{-10} & \text{expt} \\ 11658471.810(0.016) + 691.6(4.6)(3.5) + 15.4(.2)(.1) \times 10^{-10} & QED + \text{hadronic} + EW \end{cases} \quad (36)$$

where the first experimental uncertainty is statistical and the second systematic. The hadronic uncertainties are from lowest and higher order. The electroweak contribution, which at one loop is

$$a_\mu^{EW,1-loop} \simeq \frac{G_F m_\mu^2}{8\sqrt{2}\pi^2} \left[ \frac{5}{3} + \frac{1}{3}(1 - 4s_W^2) \right] \quad (37)$$

includes the two loop effects (a  $\sim 25\%$  correction), and the electroweak uncertainties are from the unknown Higgs mass and quark loop effects. The difference between experiment and theory is

$$\Delta a_\mu = a_\mu^{exp} - a_\mu^{SM} = 29.2(6.3)(5.8) \times 10^{-10} \quad (38)$$

so when we ask our model to “fit the  $(g-2)_\mu$  discrepancy”, we will ask it to contribute  $\delta a_\mu \sim a_\mu^{EW} \sim +15 \times 10^{-10}$  to the theoretical calculation of  $a_\mu$ .

We now calculate the bounds from a selection of one and two loop diagrams contributing to  $(g-2)_\mu$  and  $\tau \rightarrow \mu\gamma$ . We aim to describe the leading constraints. The model we consider has many unknown Yukawa interactions, so which diagrams give the most “interesting” limits depends on what is assumed about the pattern of Yukawa couplings. For instance, a two-loop diagram that is linear in a small Yukawa coupling can give a more significant bound than a one loop diagram that is quadratic in that same Yukawa coupling [17]. Various theoretically motivated patterns for the Yukawas have been discussed in the literature [40, 41, 66], and many analyses concentrate on the supersymmetric case, where the flavour-violating Yukawas are loop induced, and  $\rho_{tt} \propto \cot \beta$ ,  $\rho_{\tau\mu} \propto \tan \beta$ .

We only include diagrams that contain the flavour changing couplings<sup>5</sup>  $\rho_{\tau\mu}$ . It appears squared in the lepton flavour conserving amplitude  $a_\mu$ , and in the lepton flavour changing rate  $\Gamma(\tau \rightarrow \mu\gamma)$ .

At one loop, three Yukawa couplings are required on the fermion line of the dipole operator, so we expect  $C^{\mu\mu} \propto |g_{\phi\tau\mu}|^2 m_\tau$  and  $C^{\mu\tau} \propto g_{\phi\tau\tau} g_{\phi\tau\mu} m_\tau$ . We do not consider possible large logs that could arise from electroweak corrections to these diagrams. We do consider two loop contributions to  $C^{\tau\mu}$  which have only one Yukawa coupling on the lepton line. The other end of the  $\phi$  propagator must attach somewhere, and an external Higgs vev is required for the dipole operator. If this pair of Higgs couplings can be large (for instance gauge, third generations Yukawas, or scalar self-interactions) they could compensate the  $1/(16\pi^2)$  relative to the one-loop diagram. Therefore we include the two-loop “Barr-Zee” diagrams (figure 1) with third generation quarks, and with  $W$  bosons. We neglect “Barr-Zee” diagrams with charged Higgses in the second loop for simplicity, and because these loops are relatively suppressed<sup>6</sup>.

Our formulae are incomplete, possibly gauge dependent (the  $W$  loop diagrams of figure 2), and we have not excluded large logs in higher loop corrections (as in the SM electroweak contribution to  $g-2$  [67]). Due to these uncertainties, we will be reluctant to exploit cancellations between diagrams.

### 4.3 g-2

There are one loop (and higher order) contributions to  $a_\mu$  mediated by the flavour conserving couplings of the 2HDM. The possibility of explaining the  $(g-2)_\mu$  discrepancy with these terms was discussed in [19], who show that there is little parameter space consistent with other constraints on the 2HDM. We assume that  $(g-2)_\mu$  does not constrain the flavour-conserving parameters of our model [57].

In the presence of the flavour changing  $\rho_{\tau\mu}$  coupling, there is a one-loop contribution to  $(g-2)_\mu$ , illustrated on the left in figure 2. As discussed above, it should be of order the one-loop electroweak gauge contribution, or

<sup>5</sup>So we neglect the flavour diagonal contributions to  $(g-2)$  — see the references at the beginning of section 4.3.

<sup>6</sup>Such diagrams could be expected to give significant contributions, because they are proportional to quartic Higgs couplings, which can be  $\sim 1$  because we have mass<sup>2</sup> differences in our Higgs spectrum  $\sim v^2$ . However, the amplitudes are suppressed by  $m_\phi^2/m_{H+}^2$ , and there is a partial cancellation between the  $H_+$  loops with both photons attached in the same place and with the two photons attached separately [22]. The  $H_+$  loops are therefore an order of magnitude smaller than the top loop, for quartic Higgs couplings  $\sim 1$ . Secondly, the relevant Higgs couplings (see eqn (9))  $\Lambda_3$  and  $\Lambda_7$ , are independent of the Higgs masses (see eqns (18) to (22)), so are free parameters which just add more confusion to the analysis. We are reluctant to allow  $|\Lambda_3|, |\Lambda_7| \gtrsim 3$ , which would allow to (partially) cancel the top loop.

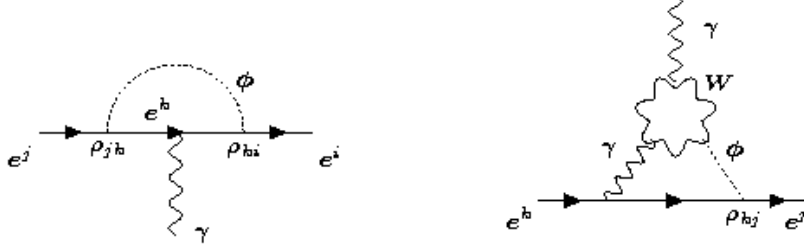


Figure 2: One and two loop diagrams, which contribute to the dipole operator coefficient  $C_{e\gamma}^{ij}$  (see eqn (33)). A mass insertion is required on the fermion line of the one loop diagram. For  $k = \tau$  and  $j = i = \mu$ , these diagrams depend only on the Yukawa couplings  $\rho_{\tau\mu}$ .

less. The chirality flip is provided by the  $\tau$  mass, which increases this diagram with respect to flavour diagonal ones. Neglecting the lepton masses in the kinematics, the one loop contribution gives [3]

$$\begin{aligned} a_\mu^{2HDM,LFV} &\simeq \sum_\phi g_{\phi\tau\mu}^2 \frac{m_\mu m_\tau}{8\pi^2} \int_0^1 dx \frac{x^2}{m_\phi^2 - x(m_\phi^2 - m_\tau^2)} \\ &\simeq \sum_\phi g_{\phi\tau\mu}^2 \frac{m_\mu m_\tau}{8\pi^2 m_\phi^2} \left( \ln \frac{m_\phi^2}{m_\tau^2} - \frac{3}{2} \right) \end{aligned} \quad (39)$$

where  $\phi = h, H, A$ , and  $g_{\phi ff'}$  is from eqn (13).

In the absence of cancellation between the opposite sign CP-even and CP-odd Higgs diagrams,

$$\kappa_{\tau\mu} \tan \beta_\tau \lesssim 32 \frac{m_\phi}{100 \text{ GeV}} \quad (40)$$

contributes at most the experiment-theory discrepancy in  $\Delta a_\mu \sim 2a_\mu^{EW}$  [3]. This bound agrees with the naive power counting expectation that  $\frac{m_\tau}{m_\mu} |\rho_{\tau\mu}|^2 / m_\phi^2 \lesssim G_F$ .

#### 4.4 $\tau \rightarrow \mu\gamma$

The two body decay  $\tau \rightarrow \mu\gamma$  can arise via loops, and the current bound on the Branching Ratio is given in eqn (35). Since the Standard Model decay  $\tau \rightarrow \ell\nu\bar{\nu}$  is three body, the bound on New Physics in a loop is particularly restrictive, because the  $|1/16\pi^2|^2$  loop factor is partially compensated by the two to three body phase space ratio.

To estimate  $BR(\tau \rightarrow \mu\gamma)$  in our model, we assume that  $A_L = A_R \equiv A$ , and neglect the lepton masses in the kinematics. We include the one-loop diagram of figure 2 (the first sum below), and a subset of two-loop diagrams. Following [22], we include the two-loop diagram of figure 1, with an internal photon and a third generation quark. This is the second sum below, with  $f = t, b$ , and is gauge invariant on its own. The remainder of eqn (41) is a subset of the two loop  $W$  diagrams (as in figure 2) [22]. The amplitude is:

$$\begin{aligned} A &\simeq \frac{1}{16\pi^2} \left( \sqrt{2} \sum_\phi \frac{g_{\phi\mu\tau} g_{\phi\tau\tau}}{m_\phi^2} \left( \ln \frac{m_\phi^2}{m_\tau^2} - \frac{3}{2} \right) \right. \\ &\quad + 2 \sum_{\phi,f} g_{\phi\mu\tau} g_{\phi ff} \frac{N_c Q_f^2 \alpha}{\pi} \frac{1}{m_\tau m_f} f_\phi \left( \frac{m_f^2}{m_\phi^2} \right) \\ &\quad \left. - \sum_{\phi=h,H} g_{\phi\mu\tau} C_{\phi WW} \frac{g\alpha}{2\pi m_\tau m_W} \left[ 3f_\phi \left( \frac{m_W^2}{m_\phi^2} \right) + \frac{23}{4} g \left( \frac{m_W^2}{m_\phi^2} \right) + \frac{3}{4} h \left( \frac{m_W^2}{m_\phi^2} \right) + m_\phi^2 \frac{f_\phi \left( \frac{m_W^2}{m_\phi^2} \right) - g \left( \frac{m_W^2}{m_\phi^2} \right)}{2m_W^2} \right] \right) \end{aligned} \quad (41)$$

where  $\phi = h, H, A$ ,  $f = t, b$ , the coupling  $g_{\phi ff'}$  of the internal loop fermion to the scalar  $\phi$  is given in eqn (13), and the scalar- $W^+W^-$  couplings  $C_{\phi WW}$  are given in eqn (7). There is a factor  $m_\tau$  in the denominator

of the two-loop expressions because it appears in the definition (34), and a factor of the loop mass because the functions  $f(z), g(z), h(z)$  are proportional to this mass<sup>2</sup>, whereas the loop has a single mass insertion.

The various functions are [22]:

$$f_A(z) \equiv g(z) = \frac{z}{2} \int_0^1 dx \frac{1}{x(1-x)-z} \ln \frac{x(1-x)}{z} \quad \text{pseudoscalar} \quad (42)$$

$$f_{h,H}(z) = \frac{z}{2} \int_0^1 dx \frac{(1-2x(1-x))}{x(1-x)-z} \ln \frac{x(1-x)}{z} \quad \text{scalars}, \quad (43)$$

and

$$h(z) = -\frac{z}{2} \int_0^1 \frac{dx}{x(1-x)-z} \left[ 1 - \frac{z}{x(1-x)-z} \ln \frac{x(1-x)}{z} \right] \quad (44)$$

They are  $\sim z$  for arguments  $z$  of order 1, and for small  $z$ ,  $f_\phi(z) \sim \frac{z}{2}(\ln z)^2$ .

The  $\tau \rightarrow \mu\gamma$  amplitude  $A$  depends on  $\tan \beta_\tau$ ,  $(\beta - \alpha)$ , and the Higgs masses. It is useful to estimate the relative size of the one-loop, two-loop fermion, and two-loop  $W$  contributions in various cases.

1. We start by estimating the one-loop diagrams contributing to  $\tau \rightarrow \mu\gamma$ . In the absence of cancellations between the opposite sign CP-even and CP-odd Higgs diagrams, the approximate  $\tau \rightarrow \mu\gamma$  bound  $|A| < 10^{-4}G_F$  gives

$$\frac{\kappa_{\mu\tau}\kappa_{\tau\tau}\tan^2\beta_\tau}{8\pi^2} \sqrt{\frac{m_\mu}{m_\tau}} \frac{m_\tau^2}{m_\phi^2} \ln \frac{m_\phi^2}{m_\tau^2} < 10^{-4} \quad (45)$$

or, for  $\kappa_{\tau\tau} \simeq 1$ :

$$\kappa_{\mu\tau}\tan^2\beta_\tau \lesssim 160 \left( \frac{100\text{GeV}}{m_\phi} \right)^2 \quad (46)$$

which is weaker than the estimated  $(g-2)$  bound of eqn (40) for small  $\tan \beta_\tau$ , and more restrictive as  $\tan \beta_\tau$  grows. In the case  $\phi = A$ , the bound (32) from  $\tau \rightarrow \eta\mu$  is more restrictive.

2. Consider now the two-loop contributions to  $\tau \rightarrow \mu\gamma$ , starting with the top loop. For small  $\tan \beta_\tau$ , or large mixing  $s_{\beta-\alpha} \sim c_{\beta-\alpha}$  between the Higgses, this can be the dominant contribution to  $\tau \rightarrow \mu\gamma$ . The ratio of the top-loop to one loop amplitudes, induced by a particular Higgs  $\phi$ , is

$$\begin{aligned} \frac{2\text{loop top}}{1\text{loop}} &\sim \frac{\alpha Q_t^2 (c_{\beta-\alpha}s_{\beta-\alpha} + \cot \beta_\tau) m_t^2}{m_\tau v m_\phi^2} \frac{m_\phi^2 v}{m_\tau \kappa_{\tau\tau} \tan \beta_\tau \ln(\frac{m_\phi}{m_\tau})} \\ &\sim \alpha Q_t^2 \frac{(c_{\beta-\alpha}s_{\beta-\alpha} + \cot \beta_\tau) m_t^2}{m_\tau^2} \frac{1}{\kappa_{\tau\tau} \tan \beta_\tau \ln(\frac{m_\phi}{m_\tau})} \end{aligned} \quad (47)$$

where  $g_{\phi ff'}$  is from eqn (13). So for  $\kappa_{\tau\tau} \sim 1$ , and  $c_{\beta-\alpha}s_{\beta-\alpha} \sim 1$ , the 2-loop top diagram dominates over the one loop for  $\tan \beta_\tau \lesssim m_t/m_b$ . This is because all the Higgses have an  $\mathcal{O}(m_t/v)$  coupling to the top, independently of  $\tan \beta_\tau$ . However, the  $c_{\beta-\alpha}s_{\beta-\alpha}$  terms of the  $h$  and  $H$  amplitudes have opposite sign (recall that  $g_{Aff'}$  is independent of  $\beta - \alpha$ ). Imposing the approximate  $\tau \rightarrow \mu\gamma$  bound  $|A| < 10^{-4}G_F$  on the top amplitude, for case 1:  $m_h \simeq m_H \ll m_A$ , and for case 2:  $m_h \simeq m_A \ll m_H$  with  $s_{\beta-\alpha} \sim 1$ , implies

$$10 \gtrsim \begin{cases} \left( \frac{m_H^2 - m_b^2}{m_h^2} \sin 2(\beta - \alpha) + \frac{1}{\tan \beta_\tau} \right) \kappa_{\tau\mu} \tan \beta_\tau & \text{case1} \\ \kappa_{\tau\mu} & \text{case2} \end{cases} \quad (48)$$

which is somewhat more restrictive than the estimated  $(g-2)$  bound of eqn (40), and one-loop  $\tau \rightarrow \mu\gamma$  bound of eqn (45). However, for large  $\tan \beta_\tau$ , small  $c_{\beta-\alpha}s_{\beta-\alpha} < \cot \beta_\tau$  and  $\kappa_{\tau\tau} \sim 1$ , the one-loop contribution is larger..

3. Superficial inspection suggests that the two loop diagrams with an internal  $b$  or  $W$  loop, never provide a dominant contribution (although they are included in our plots). Parametrically, the two loop contributions of the  $t$ ,  $W$  and  $b$  give the following three terms

$$\frac{\kappa_{\tau\mu} \tan \beta_\tau}{m_\phi^2} \left( N_c Q_t^2 m_t^2 [c_{\beta-\alpha}s_{\beta-\alpha} + \cot \beta_\tau] + c_{\beta-\alpha}s_{\beta-\alpha} m_W^2 + N_c Q_b^2 m_b^2 \tan \beta_\tau \ln(\frac{m_\phi}{m_b}) \right) \quad (49)$$

so one sees that the  $W$  loop can be neglected with respect to the tops. Notice from eqns (13) and (7), that when  $s_{\beta-\alpha}$  or  $c_{\beta-\alpha}$  is small, one of  $h$  or  $H$  is “SM-like”, meaning that it has coupling  $\sim gm_W$  to  $W^+W^-$ , flavour-diagonal couplings  $\sim m_f/v$  to the fermions, and suppressed flavour-changing interactions. So the effective interaction of  $W^+W^-\tau\bar{\mu}$ , induced by the neutral Higgses, is  $\propto \sin 2(\beta - \alpha)$ . Similarly, the Higgs-induced  $t\bar{t}\tau\bar{\mu}$  is  $\propto \sin 2(\beta - \alpha) + \mathcal{O}(\rho_{\phi tt})$ . This is in accordance with [22], who observe that the  $W$  loop contribution vanishes in the decoupling limit due to unitarity arguments. It disagrees with the MSSM analysis of [68], where the  $W$  contribution is included but the tops are not.

Comparing the one loop amplitude to the two loop bottom amplitude, for large  $\tan \beta_\tau < 1/(c_{\beta-\alpha}s_{\beta-\alpha})$  when the  $b$  loop could dominate the top, one obtains:

$$\frac{1loop}{2loop\ bottom} \sim \frac{\kappa_{\tau\tau} \tan \beta_\tau m_\tau \ln(\frac{m_\phi}{m_\tau})}{vm_\phi^2} \frac{m_\tau vm_\phi^2}{\alpha Q_b^2 m_b^2 \tan \beta_\tau \ln(\frac{m_\phi}{m_b})} \sim \frac{\kappa_{\tau\tau} m_\tau^2}{\alpha Q_b^2 m_b^2} \quad (50)$$

This suggests that unless  $\kappa_{\tau\tau} \ll 1$ , the one-loop contribution is larger than the two-loop when  $1/(c_{\beta-\alpha}s_{\beta-\alpha}) > \tan \beta_\tau \gtrsim 3$ .

- Finally, recall that cancellations can occur in the sum. There is a relative negative sign between the CP-even and CP-odd Higgs diagrams (which has little effect in many of our plots because we set  $m_A \simeq m_{H^+} \simeq 300$  GeV, to minimise the  $T$  parameter), and also between the  $h$  and  $H$  induced two loop top amplitudes at negligible  $\cot \beta_\tau$ , which would cancel for  $m_h^2 = m_H^2$ .

The bound on  $\kappa_{\tau\mu} \tan \beta_\tau$  from  $\tau \rightarrow \mu\gamma$  is plotted in figure 3, for  $m_h = 117$  GeV,  $m_H = 130$  GeV,  $m_{H^+} = 300$  GeV,  $|m_A - m_{H^+}| = 10$  GeV, and  $\kappa_{\tau\tau} = 1$ . As expected, for  $\tan \beta_\tau \gtrsim$  few and small  $\sin(\beta - \alpha)$ , the amplitude is dominated by the one-loop contribution, and the constraint on  $\kappa_{\tau\mu} \tan \beta_\tau$  scales as  $1/\tan \beta_\tau$  for fixed  $\beta - \alpha$ .

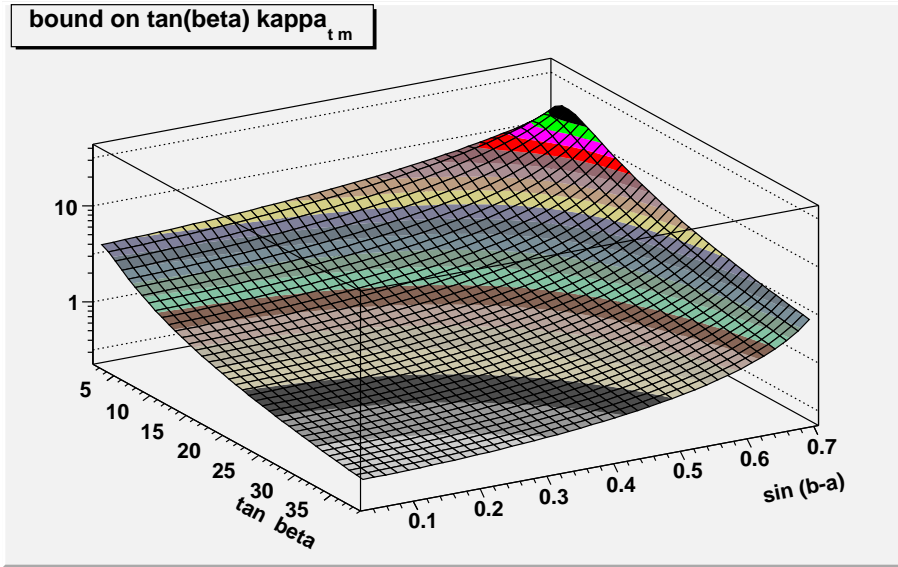


Figure 3: Bound on  $\kappa_{\tau\mu} \tan \beta_\tau$  from the experimental limit on  $BR(\tau \rightarrow \mu\gamma)$ , as a function of  $\tan \beta_\tau$  and  $\sin(\beta - \alpha)$ , for  $m_h = 117$  GeV,  $m_H = 130$  GeV,  $m_{H^+} = 300$  GeV and  $|m_A - m_{H^+}| < 20$  GeV. We take  $\kappa_{\tau\tau} = 1$ .

The relative importance of the  $(g - 2)$  and  $\tau \rightarrow \mu\gamma$  constraints is illustrated in figure 4, for a particular choice of Higgs masses. The two loop contributions to  $\tau \rightarrow \mu\gamma$  (discussed above) are also included in this plot. For  $\kappa_{\tau\mu} = 1$ , the double ratio of the predicted  $a_\mu^{2HDM,LFV}$  from eqn (39) over the  $(g - 2)$  discrepancy (taken to be  $15 \times 10^{-10}$ ), is divided by the predicted  $\tau \rightarrow \mu\gamma$  branching ratio over the current bound:

$$\frac{\frac{a_\mu^{2HDM,LFV}}{\Delta a_\mu}}{\frac{BR^{2HDM,LFV}(\tau \rightarrow \mu\gamma)}{BR^{data}(\tau \rightarrow \mu\gamma)}} \quad (51)$$

Since both predictions scale as  $|\rho_{\tau\mu}|^2$ , this cancels in the ratio, which therefore quantifies the relative significance of the bounds. Since the ratio  $< 1$ , we conclude that for generic mass choices that give a small  $T$

parameter, it is not possible to take  $\rho_{\tau\mu}$  large enough to fit  $(g-2)_\mu$ , without exceeding the bound from  $\tau \rightarrow \mu\gamma$ . The plot is obtained by a grid scan. We consider  $\beta - \alpha : 0 \rightarrow \pi/4$ , because the range  $\pi/4 \rightarrow \pi/2$  is equivalent if one simultaneously exchanges <sup>7</sup>  $m_h$  and  $m_H$ .

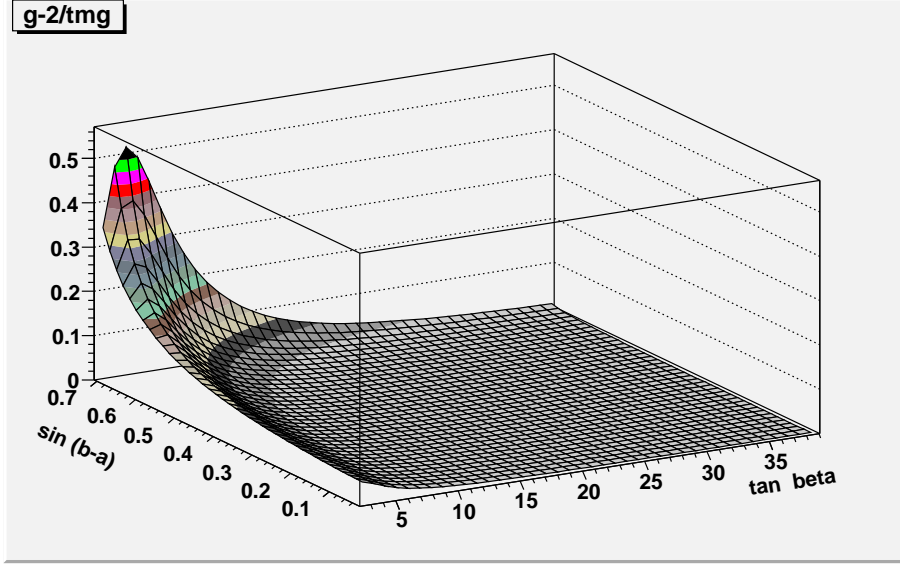


Figure 4: The double ratio, given in eqn (51), of the contribution to  $(g-2)_\mu$  divided by half the experimental discrepancy, over the contribution to  $\tau \rightarrow \mu\gamma$  divided by its experimental limit. It is plotted as a function of  $\tan\beta_\tau$  and  $\sin(\beta - \alpha)$ , for  $m_h = 117$  GeV,  $m_H = 130$  GeV,  $m_{H^+} = 300$  GeV, and  $|m_{H^+} - m_A| = 10$  GeV. Both contributions are  $\propto (\kappa_{\tau\mu} \tan\beta_\tau)^2$ , which cancels in the ratio. Assuming that our mass choices are representative, this shows that the current experimental bound on  $\tau \rightarrow \mu\gamma$  is more restrictive than  $(g-2)_\mu$ .

## 4.5 Assumptions about the $\rho_{ff}$

As previously mentioned, the bounds on  $\rho_{\tau\mu}$  depends on the assumptions made for the other model parameters, such as  $\rho_{\tau\tau}$ ,  $\rho_{tt}$ ,  $\rho_{bb}$ , and the Higgs masses. We focus on three limits.

The most conservative approach to setting bounds on  $\rho_{\tau\mu}$ , is to neglect all other couplings. In this case, the  $(g-2)$  bound will hold, and vary as a function of the neutral Higgs masses, but the  $\tau \rightarrow \mu\gamma$  bound plotted in figure 3 does not apply because it assumed  $\rho$  matrices as given in eqn (16). Neglecting the flavour diagonal Yukawa couplings of the flavour violating  $\phi$ , is equivalent to setting them to zero. So this case corresponds to  $c_{\beta-\alpha} = 0$ , where one CP-even Higgs ( $h$ ) is SM-like, and both  $H$  and  $A$  have the flavour-violating  $\rho_{\tau\mu}$  coupling, but no tree-level interactions with  $ts$ ,  $bs$  or  $Ws$ . Such additional Higgses would be difficult to produce at colliders, so we do not consider further this case.

We are interested in a Higgs that could be copiously produced at hadron colliders in  $gg$  fusion. This can be obtained by allowing the flavour-violating Higgs an  $\mathcal{O}(1)$  Yukawa coupling to the top. This is realised for  $\sin 2(\beta - \alpha) \sim 1$ , in the parametrisation of Yukawa couplings given in eqns (13) and (16). In this case, the top loop contribution to  $\tau \rightarrow \mu\gamma$  (see figure 1) is significant at small  $\tan\beta_\tau$ , as discussed in section 4.4 and the diagram for the  $gg \rightarrow \tau\bar{\mu}$  process at colliders is closely related to the  $\tau \rightarrow \mu\gamma$  diagrams, as expected from the diagrams in figure 1.

Finally, consider the large  $\tan\beta_\tau$  limit. Recall that we defined  $\tan\beta_\tau$  in our type III model using the tau Yukawa coupling (see eqn (15)). Then we assumed that all the other fermions shared this definition of  $\tan\beta_\tau$ , and had type II Yukawa interactions. Such “almost Type II” couplings could arise in Supersymmetry, where the flavour violating Yukawas grow in the large  $\tan\beta$  limit [26]. For large  $\tan\beta_\tau$ , the bound on  $\kappa_{\tau\mu} \tan\beta_\tau$  arises from the one loop contributions to  $\tau \rightarrow \mu\gamma$ , and is (approximately) independent of  $\sin 2(\beta - \alpha)$ . However, the Higgs-induced  $\bar{t}t\tau\bar{\mu}$  interaction is  $\propto \sin 2(\beta - \alpha)$ , so, as we will see in the next section,  $gg \rightarrow \phi \rightarrow \tau^\pm \mu^\mp$  is suppressed at small  $\sin 2(\beta - \alpha)$ . This can be seen by comparing figures 5 and 3 at small<sup>8</sup>  $s_{\beta-\alpha}$ .

<sup>7</sup>The Higgs couplings are unchanged if one interchanges  $h$  with  $H$ , and simultaneously  $(\beta - \alpha) \rightarrow (\beta - \alpha) - \pi/2$ . And since  $h$  and  $H$  are summed in the amplitude  $\mathcal{A}$ :  $\mathcal{A}(c_{\beta-\alpha} \rightarrow 0) = \mathcal{A}(s_{\beta-\alpha} \rightarrow 0) + \text{corrections due to } m_H^2 \neq m_h^2$ .

<sup>8</sup>Small  $\sin 2(\beta - \alpha)$  can be obtained because either  $s_{\beta-\alpha}$  or  $c_{\beta-\alpha}$  is small. Both cases are discussed in the supersymmetric

## 4.6 Summary

For much of the parameter space of this model, the bound from  $\tau \rightarrow \mu\gamma$  precludes explaining the  $g-2$  discrepancy (see figure 4). We will see in the following section, that generic 2HDM parameters giving a detectable rate for  $p\bar{p} \rightarrow \phi \rightarrow \tau^\pm \mu^\mp$  in current Tevatron data are already excluded by precision bounds. However, a signal at the Tevatron could arise if there are cancellations in the  $\tau \rightarrow \mu\gamma$  amplitude.

## 5 Colliders

The leading order production cross-section of Higgses, by gluon-gluon fusion at a  $p\bar{p}$  collider, is [9]

$$\sigma_{LO}(p\bar{p} \rightarrow \phi) = \frac{G_F \alpha_s^2 m_\phi^2}{288 \sqrt{2} \pi s} \left| \frac{3}{4} \sum_{q=t,b} g_{\phi qq} \mathcal{A}^\phi(z_q) \right|^2 \int_{z_\phi}^1 \frac{dx}{x} g(x) g(x/z_\phi) \quad (52)$$

where  $z_\phi = m_\phi^2/s$ ,  $z_q = (4m_q^2)/m_\phi^2$ , the gluon density in the proton (or anti-proton) is  $g(x)$ ,

$$\mathcal{A}^{h,H}(z) = 2z[1 + (1-z)f(z)] \quad (53)$$

$$\mathcal{A}^A(z) = 2zf(z) \quad (54)$$

and

$$f(z) = \begin{cases} \arcsin^2 \sqrt{\frac{1}{z}} & z \geq 1 \\ -\frac{1}{4} \left[ \log \frac{1+\sqrt{1-z}}{1-\sqrt{1-z}} - i\pi \right]^2 & z < 1 \end{cases} \quad (55)$$

The next order QCD corrections to the production cross section are  $\sim 20 - 90\%$ , and can be mimicked by a K factor [9]. Finally, to obtain the cross-section for  $p\bar{p} \rightarrow \tau\bar{\mu}$ , the cross-section (52) should be multiplied by the branching ratio  $BR(\phi \rightarrow \tau\bar{\mu})$ .

The Tevatron searches for SM Higgses, decaying to  $\tau\bar{\tau}$ , in the mass range 105- 145 GeV [72, 73]. A recent D0 analysis [73] obtains limits on the cross-section  $\times$  branching ratio of order  $20-90 \times$  the SM expectation. If we imagine that the  $\tau\bar{\mu}$  final state is detectable with similar efficiencies to  $\tau\bar{\tau}$ , then the parameters to which the Tevatron is sensitive can be estimated as follows. We normalise the  $\phi$  production cross-section and branching ratio to the SM expectation for  $h_{SM} \rightarrow \tau^+ \tau^-$ :

$$R_\phi^\sigma \equiv \frac{\sigma_{LO}(p\bar{p} \rightarrow \phi)}{\sigma_{LO}(p\bar{p} \rightarrow h_{SM})} = \frac{\left| \frac{3}{4} \sum_{q=t,b} g_{\phi qq} \mathcal{A}^\phi(z_q) \right|^2}{\left| \frac{3}{4} \frac{gm_t}{2m_W} \mathcal{A}^h(z_t) \right|^2} \quad (56)$$

$$\begin{aligned} R_\phi^{BR} &\equiv \frac{BR(\phi \rightarrow \tau\bar{\mu}, \mu\bar{\tau})}{BR(h_{SM} \rightarrow \tau\bar{\tau})} \\ &\simeq \frac{2\kappa_{\tau\mu}^2 \tan^2 \beta_\tau m_\mu / m_\tau}{\left| \frac{v}{m_\tau} g_{\phi\tau\tau} \right|^2 (1 - B_{2W}) + |c_{\phi WW}|^2 B_{2W}} \times \begin{cases} s_{\beta-\alpha}^2 & \phi = h \\ c_{\beta-\alpha}^2 & \phi = H \\ 1 & \phi = A \end{cases} \end{aligned} \quad (57)$$

where  $h_{SM}$  is the Standard Model higgs,  $m_{h_{SM}}$  is taken to be equal to  $m_\phi$  and  $B_{2W} = BR(h_{SM} \rightarrow W^+ W^-)$  which varies with  $m_h$ . We estimate that

$$R_\phi^\sigma R_\phi^{BR} \lesssim 30 \quad (58)$$

because the Tevatron limit on  $\sigma(p\bar{p} \rightarrow h_{SM} \rightarrow \tau\bar{\tau})$  is  $\sim 20 - 90 \times$  the SM expectation<sup>9</sup>. In the large  $m_A$  scenario, where the Tevatron would be looking for a CP-even  $\phi$ , our lepton flavour violating rate is maximised for large  $\sin 2(\beta - \alpha) \sim 1$  and small  $\tan \beta_\tau = 2$ . The Tevatron bound would be of order

$$\kappa_{\tau\mu} \tan \beta_\tau \lesssim \sqrt{\frac{m_\tau}{m_\mu}} (20 \text{ to } 90) \sim 20 \quad (59)$$

which is on the border of the exclusion estimate from  $\tau \rightarrow \mu\gamma$ , given in eqns(45) and (48). In the large  $m_H$  scenario, where  $s_{\beta-\alpha} \rightarrow 1$ , the Tevatron could look also for  $A \rightarrow \tau^\pm \mu^\mp$ . At small  $\tan \beta_\tau$ , the production rate is

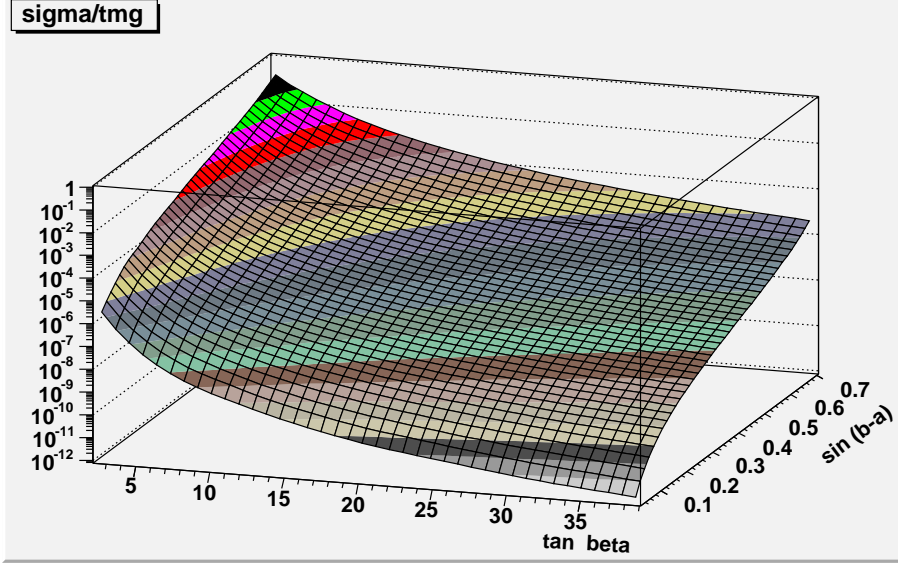


Figure 5: Estimate of the relative sensitivity of  $\sigma(p\bar{p} \rightarrow h \rightarrow \tau^\pm \mu^\mp)$  and  $\tau \rightarrow \mu\gamma$  to  $\rho_{\tau\mu}$  from current data. The plot is the double ratio of  $R_h^\sigma R_h^{BR}$  (see eqns 57 and 56) over  $BR(\tau \rightarrow \mu\gamma)$ , divided by current experimental limits (see eqns (35) and (58)), as a function of  $\tan\beta_\tau$  and  $\sin(\beta - \alpha)$  ( $\kappa_{\tau\mu} \tan\beta_\tau$  cancels in the ratio). The plot is for  $h$  production at colliders, with  $m_h = 115$  GeV,  $m_H = 130$  GeV,  $m_{H^+} = 300$  GeV and  $|m_A - m_{H^+}| = 10$  GeV. Since the ratio  $< 1$ ,  $\tau \rightarrow \mu\gamma$  is more sensitive. Alternatively, this plot indicates the amount of tuning required in the  $\tau \rightarrow \mu\gamma$  rate to accommodate a signal for  $h \rightarrow \tau\mu$  at the TeVatron in the near future.

similar to the standard model, so the bound should be of order eqn (59); for large  $\tan\beta_\tau$ ,  $A$  production in  $gg$  fusion is suppressed.

A more credible estimate of the relative sensitivity of colliders and  $\tau \rightarrow \mu\gamma$  to the parameter  $\kappa_{\tau\mu} \tan\beta_\tau$ , could be obtained from a double ratio, as discussed for  $(g-2)$  and  $\tau \rightarrow \mu\gamma$  at the end of section 4.4. We plot in figure 5 the double ratio of  $R_h^\sigma R_h^{BR}/[\text{the current bound on } h_{SM} \rightarrow \tau\bar{\tau}]$ , divided by the predicted  $BR(\tau \rightarrow \mu\gamma)$  normalised to its current experimental bound. Both rates are  $\propto (\kappa_{\tau\mu} \tan\beta_\tau)^2$ , so this cancels out of the ratio. This plot is made for the production, and decay to  $\tau^\pm \mu^\mp$ , of a CP even Higgs  $h$  of mass 115 GeV, with  $m_H = 130$  GeV,  $m_{H^+} = 300$  GeV and  $|m_A - m_{H^+}| = 10$  GeV. If  $m_A \simeq m_{H^+} \gtrsim 250$  GeV for B physics and the T parameter, then the current bound from  $\tau \rightarrow \mu\gamma$  makes it difficult to detect  $h \rightarrow \tau\bar{\mu}$  at the TeVatron<sup>10</sup>. The sensitivity to  $H \rightarrow \tau\bar{\mu}$  is worse, in the interesting  $\sin(\beta - \alpha) \sim \cos(\beta - \alpha) \sim \tan\beta_\tau$  region, due to sums and differences among these angles all of the same orders. However, a hadron collider able to detect  $h_{SM} \rightarrow \tau\bar{\tau}$  (an improvement of  $\sim 30$  with respect to the current Tevatron limit), would be more sensitive than  $\tau \rightarrow \mu\gamma$  in the  $\sin 2(\beta - \alpha) \gtrsim 1/2$  and small  $\tan\beta_\tau$  region. Also, cancellations are possible in the  $\tau \rightarrow \mu\gamma$  amplitude, which would increase the sensitivity of colliders relative to rare decays.

There are dubious approximations in obtaining this plot. We neglect the contribution of the  $\phi \rightarrow \tau\bar{\mu}$  decay in computing the total  $\phi$  decay rate (this approximation was also used to obtain eqn (59)). We make this overestimate of the branching ratio, so as to obtain a formula which is  $\propto |g_{\phi\tau\mu}|^2$ , so easy to compare to  $BR(\tau \rightarrow \mu\gamma)$ . It is reasonable where  $\tau \rightarrow \mu\gamma$  imposes  $\kappa_{\tau\mu} \tan\beta_\tau \lesssim 3$  (because then  $\Gamma(\phi \rightarrow \tau\bar{\mu}) \lesssim \Gamma(h \rightarrow \tau\bar{\tau})$ , and the contribution to the total decay rate is not too important); however, in the interesting small  $\tan\beta_\tau$  and large  $\sin 2(\beta - \alpha)$  region, it could overestimate  $\sigma(p\bar{p} \rightarrow h \rightarrow \tau^\pm \mu^\mp)$  by a factor  $\sim 2$  (see figure 3). A second doubtful approximation is that the higher order QCD corrections cancel in eqn (57). This may be acceptable when  $\phi$  and  $h_{SM}$  are emitted from a top loop, but in the large  $\tan\beta_\tau$  limit, the  $b$  loop can also be important for  $\phi$  production, and its NLO corrections are different. Finally, the experimental bound we use from the search for  $h_{SM} \rightarrow \tau\bar{\tau}$ [73], allows for several Higgs production mechanisms: associated production with a  $W$  or  $Z$ , vector boson fusion, or gluon fusion, and assumes a final state of  $\tau\bar{\tau} + 2$  jets. Whereas in (57), we assume production by gluon fusion.

analysis of [68]. Recall that  $c_{\beta-\alpha} \rightarrow 0$  in the decoupling limit [33], where  $A, H$  and  $H^+$  are “heavy” ( $\gtrsim 2m_W$ ), and the light higgs  $h$  has almost SM couplings.

<sup>9</sup>we use figures from table VI of [73], obtained with  $\sim 5fb^{-1}$  of data

<sup>10</sup>To rescale this plot for the LHC is straightforward: multiply by the TeVatron limit of  $\simeq 30\times$  SM expectation for  $h_{SM} \rightarrow \tau^+\tau^-$ , and divide by the LHC limit on  $\sigma(gg \rightarrow \phi \rightarrow \tau^\pm \mu^\mp)/\sigma(gg \rightarrow h_{SM} \rightarrow \tau^+\tau^-)$ .

We can also compare our prediction to bounds [74] on a MSSM Higgs produced via gluon fusion, and decaying to  $\tau^+\tau^-$ . This analysis assumed one  $\tau$  decaying hadronically and the other one to a muon and neutrinos. The cross section limits on  $\sigma \times BR(\phi \rightarrow \tau\tau)$  displayed in figure 5 of [74] indicate the current TeVatron limit on  $gg \rightarrow \phi \rightarrow \tau\mu$ . In  $\phi \rightarrow \tau^\pm\mu^\mp$ , the muon is directly produced in the decay of the Higgs, rather than from a  $\tau$ , so the signal would have a global detection efficiency roughly 5 times higher than the signal of [74], due to the absence of the factor 0.17 coming from the decay rate of  $\tau$  in  $\mu$ . So the y-axis in figure 5 of [74] could roughly be labelled as  $\sigma \times BR(\phi \rightarrow \tau\mu)/0.17$ . For a Higgs of 115 GeV, this gives a limit around 30 times the SM expectation, which is similar to the limit quoted in [73] with twice the luminosity.

For experimental bounds, we have extrapolated the potential reach of  $h \rightarrow \tau\mu$  searches from the published searches for  $h \rightarrow \tau\tau$ . In [3], it has been shown that by using appropriate cuts, it was possible to distinguish between  $h \rightarrow \tau\mu$  and  $h \rightarrow \tau\tau$  signals (see figures 13 and 14 in [3]). Various cuts can help extract a  $h \rightarrow \tau\mu$  signal from the standard model backgrounds that are still selected by a  $h \rightarrow \tau\tau$  analysis. Increasing the muon Pt threshold is a first option. In [3], this threshold is at 20 GeV, already above the thresholds used in  $h \rightarrow \tau\tau$  searches (10 GeV for CdF and 15 GeV for D0 [75]). With Higgs mass above 100 GeV, increasing the threshold up to 30 GeV can safely be done. Figure 1 of [74] shows that threshold increase would greatly reduce the amount of standard model backgrounds remaining in a  $h \rightarrow \tau\tau$  analysis. The dominant remaining backgrounds would be  $Z \rightarrow \tau\tau$ ,  $Z \rightarrow \mu\mu$ <sup>11</sup> and  $W$ +jets.

Another potentially efficient variable to isolate  $h \rightarrow \tau\mu$  signal is the effective transverse mass of the tau mu system as defined in equation (30) of [3]. For  $W$  and  $Z$  background, this variable would peak at the  $W/Z$  mass while for higgs signal, it would peak at the higgs mass (see figure 11 of [3]). Hence, a cut on this variable could further reduce the background especially for higher higgs masses.

Compared to the  $h \rightarrow \tau\tau$  analysis, a dedicated  $h \rightarrow \tau\mu$  analysis could then have fewer background events for a similar selection efficiency leading to sensitivity and limits which would be better than the one crudely extrapolated from current experimental limits on  $h \rightarrow \tau\tau$  searches [73, 74].

## 6 Summary

At hadron colliders, an interesting signature of New Physics would be the production of a neutral Higgs  $\phi$ , followed by its decay to  $\tau^\pm\mu^\mp$ . For  $m_\phi \ll 2m_W$ , the branching ratio can be large, and the process could arise in a wide variety of models. Such New Physics is constrained by precision observables, and the upper bounds on rare decays such as  $\tau \rightarrow \mu\gamma$ . In this paper, we are interested in the implications for collider searches of these loop contributions.

We parametrise the New Physics at mass scales  $\lesssim 400$  GeV, as a (CP- conserving) 2 Higgs Doublet Model (2HDM) of Type III, meaning that we allow our neutral Higgses to have the tree-level lepton flavour changing couplings of eqn (12):

$$\sim \kappa_{\tau\mu} \tan \beta_\tau \sqrt{\frac{m_\mu m_\tau}{v^2}} (c_{\beta-\alpha} h - s_{\beta-\alpha} H + iA) \bar{\tau} \mu$$

Our choices of notation, basis in Higgs space,  $\tan \beta_\tau$ , and parametrisation are discussed in section 2. We will quote and plot bounds on  $\kappa_{\tau\mu} \tan \beta_\tau$ , to avoid artificially strong bounds on  $\kappa_{\tau\mu}$  at large  $\tan \beta_\tau$ . We study the phenomenological constraints on this model: we admit arbitrary New Physics at scales  $\sim$  TeV, and retain the constraints on the 2HDM arising from the  $T$  parameter,  $b \rightarrow s\gamma$ ,  $(g-2)_\mu$  and  $\tau \rightarrow \mu\gamma$ .

The  $T$  parameter and  $b \rightarrow s\gamma$  restrict the flavour-independent parameters (masses) of the model. The charged Higgs of the 2HDM gives a significant same-sign contribution to the Standard Model (SM) amplitude for  $b \rightarrow s\gamma$  (see sect 3.2). For  $m_{H^\pm} \gtrsim 250 - 300$  GeV, this contribution is within current experimental error. In this paper, we assume such a heavy  $H^\pm$ ; this has little effect on the neutral Higgses we are interested in. The  $T$  parameter, discussed in section 3.1.4, is the sum of many terms of different sign. One way to ensure that it is small enough is to take  $m_A \sim m_{H^\pm}$ , as we assume for most of the plots. However, other cancellations are possible within the 2HDM (such as  $m_H \sim m_{H^\pm}$  with  $\sin(\beta - \alpha) \rightarrow 1$ ), or additional new light particles (such as arise in supersymmetric models) could contribute to  $T$ .

The decay  $\tau \rightarrow \mu\gamma$  and the anomalous magnetic moment of the muon  $(g-2)_\mu$  constrain the flavour-changing coupling  $\kappa_{\tau\mu} \tan \beta_\tau$ , and are discussed in sections 4.3 and 4.4. The neutral Higgses  $h, H$  and  $A$  contribute to  $(g-2)_\mu$  at one loop, with a flavour-changing coupling at both vertices, and chirality-flip via a  $\tau$  mass insertion. One could hope to fit the  $(g-2)_\mu$  discrepancy, with a 2HDM containing the  $\kappa_{\tau\mu}$  coupling, but this would require cancellations in the generically more restrictive  $\tau \rightarrow \mu\gamma$  bound (see figure 4 and eqns (40), (45) and (48)).

---

<sup>11</sup>not considered in [3]



There are relevant contributions to  $\tau \rightarrow \mu\gamma$  at one and two-loop; some diagrams are shown in figures 1 and 2. The one loop amplitude scales <sup>12</sup> as  $\frac{m_\tau^2}{v^2} \tan^2 \beta_\tau (\kappa_{\tau\mu} \tan \beta_\tau)^2$ , and does not vanish for  $\sin 2(\beta - \alpha) \rightarrow 0$ . The amplitude due to  $A$  exchange is of opposite sign from the  $h$  and  $H$  amplitudes, so the one-loop contribution to  $\tau \rightarrow \mu\gamma$  can be suppressed by tuning similar masses for  $h, H$  and  $A$ . Notice however, that the tuning required becomes finer with increasing  $\tan \beta_\tau$ , so at large  $\tan \beta_\tau$ ,  $\tau$  decays are a more sensitive probe [5] of  $\kappa_{\tau\mu} \tan \beta_\tau$  than hadron colliders. See [76] for a discussion of the promising prospects at an  $e - \gamma$  collider.

The two-loop ‘‘Barr-Zee’’ contributions to  $\tau \rightarrow \mu\gamma$  can be of the same order as the one loop. The effective dipole interaction of  $\tau, \mu$  and  $\gamma$ , must contain at least three Yukawa couplings at any loop order; if the Higgs has  $\mathcal{O}(1)$  couplings to the tops, then two of the three Yukawa couplings in the two-loop diagram can be top Yukawas. At large  $\tan \beta_\tau$ , the  $\phi$ -induced effective interaction  $\bar{t}t\bar{\tau}\mu$  vanishes with  $\sin 2(\beta - \alpha)$ . In this  $\sin 2(\beta - \alpha) \rightarrow 0$  limit, one of  $h$  and  $H$  becomes ‘‘Standard-Model-like’’, with large couplings to the  $t$  and  $W$ , while  $A$  and the other CP-even scalar have unsuppressed flavour-changing interactions. However, as illustrated in figure 1, the ‘‘Barr-Zee’’ diagrams are closely related to Higgs production by gluon fusion. So if the contribution to  $\tau \rightarrow \mu\gamma$  is suppressed in this way, the collider cross-section is suppressed as well. The two loop top diagrams tend to dominate the  $\tau \rightarrow \mu\gamma$  amplitude at small  $\tan \beta_\tau$  and large  $\sin 2(\beta - \alpha)$ . Their contribution can be suppressed by cancellations between diagrams — for instance the  $h$  amplitude cancels against the  $H$  amplitude when  $1/\tan \beta_\tau \rightarrow 0$  and  $m_h \rightarrow m_H$  — but these cancellations do not arise for the same parameter choices as suppress the one loop amplitude.

So in practise, the model is described by  $m_{H+}$  (taken  $\simeq 300$  GeV to satisfy  $b \rightarrow s\gamma$ ),  $m_h (\simeq 114$  GeV),  $m_A$  and  $m_H$  (one of which should be ‘‘light’’ to avoid the decoupling limit, and the the  $T$  parameters constraint can be satisfied if the other is heavy),  $\tan \beta_\tau$  ( $\sim$  few, to maximise Higgs production by gluon fusion at the Tevatron and the LHC), and  $\sin(\beta - \alpha)$  (which is unconstrained if  $m_A \simeq m_{H+}$ , and is constrained to be  $\sim 1$  by the  $T$  parameter if  $m_H \simeq m_{H+}$ ). Despite the freedom to vary  $\sin(\beta - \alpha)$ , we find it difficult to generate a detectable cross-section at the Tevatron with parameters that satisfy the precision constraints.

In the absence of cancellations,  $\tau \rightarrow \mu\gamma$  is a more sensitive probe of the  $\kappa_{\tau\mu}$  coupling, than  $\phi \rightarrow \tau^\pm \mu^\mp$  at the Tevatron with  $\sim 5/\text{fb}$  data. This can be seen from figure 5. However, it is possible to evade constraints that arise from loops by tuning parameters, or by adding (more) New Physics. We have not studied this, for reasons of principle and practise. Our approach is phenomenological, so tuning masses and mixing angles to cancel one and two loop contributions appears ad hoc. In a model, cancellations can be justified by symmetries. More practically, we do not use complete gauge invariant two loop formulae, and do not have an estimate for higher order effects, so cancellations we find might not persist in a better analysis.

Direct collider searches can give clearer bounds, being less dependent than loop processes on the vagaries of cancellations. Multiplying figure 5 by the current Tevatron bound on  $\sigma(p\bar{p} \rightarrow h_{SM} \rightarrow \tau^+\tau^-)$  which is  $\sim 30\sigma_{SM}$ , shows that  $\sigma(gg \rightarrow h \rightarrow \tau^\pm \mu^\mp)$  can be of order  $\sigma(gg \rightarrow h_{SM} \rightarrow \tau^+\tau^-)$ , and consistent with  $\tau \rightarrow \mu\gamma$  (for small  $\tan \beta_\tau$ ). So observing  $\phi \rightarrow \tau^\pm \mu^\mp$  in the near future would require ‘‘tuning’’ by the ratio plotted in figure 5: a factor  $\sim .1$  for small  $\tan \beta_\tau$ .

## References

- [1] E. O. Iltan, Phys. Rev. D **64** (2001) 013013 [arXiv:hep-ph/0101017].
- [2] R. Diaz, R. Martinez and J. A. Rodriguez, Phys. Rev. D **63** (2001) 095007 [arXiv:hep-ph/0010149].  
Y. F. Zhou, J. Phys. G **30** (2004) 783 [arXiv:hep-ph/0307240].
- [3] K. A. Assamagan, A. Deandrea and P. A. Delsart, Phys. Rev. D **67** (2003) 035001 [arXiv:hep-ph/0207302].
- [4] S. Arcelli, Eur. Phys. J. C **33** (2004) S726.
- [5] S. Kanemura, T. Ota and K. Tsumura, Phys. Rev. D **73** (2006) 016006 [arXiv:hep-ph/0505191].
- [6] W. Li, Y. Ma, G. Liu and W. Guo, arXiv:0812.0727 [hep-ph].
- [7] T.D.Lee, Phys. Rev. D **8** (1973) 1226; G.C. Branco, Phys. Rev. D **22** (1980) 2901.
- [8] J. F. Gunion, H. E. Haber, G. L. Kane and S. Dawson, ‘‘The Higgs Hunters Guide,’’ Addison-Wesley.

---

<sup>12</sup>This scaling is with our choice  $\tan \beta_\tau$  factors in the lepton flavour violating coupling. Other authors [68, 5] take this coupling  $\propto 1/\cos^2 \beta$ , and find a branching ratio  $\propto \tan^6 \beta$ .

- [9] A. Djouadi, Phys. Rept. **457** (2008) 1 [arXiv:hep-ph/0503172].  
A. Djouadi, Phys. Rept. **459** (2008) 1 [arXiv:hep-ph/0503173].
- [10] V. Barger, H. E. Logan and G. Shaughnessy, Phys. Rev. D **79** (2009) 115018 [arXiv:0902.0170 [hep-ph]].
- [11] W. Grimus, L. Lavoura, O. M. Ogreid and P. Osland, J. Phys. G **35** (2008) 075001 [arXiv:0711.4022 [hep-ph]]. W. Grimus, L. Lavoura, O. M. Ogreid and P. Osland, Nucl. Phys. B **801** (2008) 81 [arXiv:0802.4353 [hep-ph]].
- [12] E. A. Paschos, Phys. Rev. D **15** (1977) 1966.  
S. L. Glashow and S. Weinberg, Phys. Rev. D **15** (1977) 1958.
- [13] C. Delaunay, C. Grojean and J. D. Wells, JHEP **0804** (2008) 029 [arXiv:0711.2511 [hep-ph]].
- [14] I. Antoniadis, E. Dudas, D. M. Ghilencea and P. Tziveloglou, arXiv:0910.1100 [Unknown].
- [15] D. Atwood, L. Reina and A. Soni, Phys. Rev. D **55** (1997) 3156 [arXiv:hep-ph/9609279].
- [16] T. Han and D. Marfatia, Phys. Rev. Lett. **86** (2001) 1442 [arXiv:hep-ph/0008141].
- [17] J. D. Bjorken, K. D. Lane and S. Weinberg, Phys. Rev. D **16** (1977) 1474.
- [18] S. M. Barr and A. Zee, Phys. Rev. Lett. **65** (1990) 21 [Erratum-ibid. **65** (1990) 2920].
- [19] K. Cheung and O. C. W. Kong, Phys. Rev. D **68** (2003) 053003 [arXiv:hep-ph/0302111].
- [20] A. W. El Kaffas, W. Khater, O. M. Ogreid and P. Osland, Nucl. Phys. B **775** (2007) 45 [arXiv:hep-ph/0605142].
- [21] Y. F. Zhou and Y. L. Wu, Eur. Phys. J. C **27** (2003) 577 [arXiv:hep-ph/0110302].
- [22] D. Chang, W. S. Hou and W. Y. Keung, Phys. Rev. D **48** (1993) 217 [arXiv:hep-ph/9302267].
- [23] A. E. Carcamo, R. Martinez and J. A. Rodriguez, Eur. Phys. J. C **50** (2007) 935 [arXiv:hep-ph/0606190].
- [24] F. J. Botella, G. C. Branco and M. N. Rebelo, arXiv:0911.1753 [Unknown].
- [25] A. Pich and P. Tuzon, Phys. Rev. D **80** (2009) 091702 [arXiv:0908.1554 [hep-ph]].
- [26] A. Brignole and A. Rossi, Phys. Lett. B **566** (2003) 217 [arXiv:hep-ph/0304081].
- [27] A. Brignole and A. Rossi, Nucl. Phys. B **701** (2004) 3 [arXiv:hep-ph/0404211].
- [28] S. Davidson and H. E. Haber, Phys. Rev. D **72** (2005) 035004 [Erratum-ibid. D **72** (2005) 099902] [arXiv:hep-ph/0504050].
- [29] I. P. Ivanov, Phys. Lett. B **632** (2006) 360 [arXiv:hep-ph/0507132].
- [30] E. Accomando *et al.*, arXiv:hep-ph/0608079.
- [31] I. P. Ivanov, Phys. Rev. D **77** (2008) 015017 [arXiv:0710.3490 [hep-ph]].
- [32] V. D. Barger, J. L. Hewett and R. J. N. Phillips, Phys. Rev. D **41** (1990) 3421. F. Mahmoudi and O. Stal, arXiv:0907.1791 [hep-ph].
- [33] J. F. Gunion and H. E. Haber, Phys. Rev. D **67** (2003) 075019 [arXiv:hep-ph/0207010].
- [34] G. C. Branco, L. Lavoura and J. P. Silva, “CP violation,” Int. Ser. Monogr. Phys. **103** (1999) 1.
- [35] A. Freitas and D. Stockinger, Phys. Rev. D **66** (2002) 095014 [arXiv:hep-ph/0205281].
- [36] N. Baro, F. Boudjema and A. Semenov, Phys. Rev. D **78** (2008) 115003 [arXiv:0807.4668 [hep-ph]].
- [37] H. E. Haber and D. O’Neil, Phys. Rev. D **74** (2006) 015018 [arXiv:hep-ph/0602242].

- [38] M. Beneke, P. Ruiz-Femenia and M. Spinrath, *JHEP* **0901** (2009) 031 [arXiv:0810.3768 [hep-ph]].
- [39] M. Gorbahn, S. Jager, U. Nierste and S. Trine, arXiv:0901.2065 [hep-ph].
- [40] T. P. Cheng and M. Sher, *Phys. Rev. D* **35** (1987) 3484.
- [41] A. Antaramian, L. J. Hall and A. Rasin, *Phys. Rev. Lett.* **69** (1992) 1871 [arXiv:hep-ph/9206205].
- [42] D. O’Neil, “Phenomenology of the Basis-Independent CP-Violating Two-Higgs Doublet Model [Dissertation],” arXiv:0908.1363 [hep-ph].
- [43] J. D. Wells, “Lectures on Higgs Boson Physics in the Standard Model and Beyond,” arXiv:0909.4541 [hep-ph].
- [44] M. Sher, *Phys. Rept.* **179** (1989) 273.
- [45] I.P. Ivanov, *Phys. Rev.* **D75** (2007) 035001.
- [46] P. M. Ferreira and D. R. T. Jones, *JHEP* **0908** (2009) 069 [arXiv:0903.2856 [hep-ph]].
- [47] P.M. Ferreira, R.Santos, A Barroso, *Phys. Lett B* **603** (2004) 219, *Phys. Lett B* **629** (2005) 114.
- [48] B. W. Lee, C. Quigg and H. B. Thacker, *Phys. Rev. D* **16** (1977) 1519.
- [49] S. Kanemura, T. Kubota and E. Takasugi, *Phys. Lett. B* **313**, 155 (1993) [arXiv:hep-ph/9303263].
- [50] I. F. Ginzburg and I. P. Ivanov, *Phys. Rev. D* **72** (2005) 115010 [arXiv:hep-ph/0508020].
- [51] H. G. J. Veltman, *Phys. Rev. D* **41** (1990) 2294.
- [52] A. G. Akeroyd, A. Arhrib and E. M. Naimi, *Phys. Lett. B* **490** (2000) 119 [arXiv:hep-ph/0006035].
- [53] C. Amsler et al. (Particle Data Group), *Physics Letters B* **667**, 1 (2008)
- [54] I. Maksymyk, C. P. Burgess and D. London, *Phys. Rev. D* **50** (1994) 529 [arXiv:hep-ph/9306267].
- [55] P. H. Chankowski, M. Krawczyk and J. Zochowski, *Eur. Phys. J. C* **11** (1999) 661 [arXiv:hep-ph/9905436].
- [56] S. Bertolini, *Nucl. Phys. B* **272**, 77 (1986).
- [57] A. Wahab El Kaffas, P. Osland and O. M. Ogreid, *Phys. Rev. D* **76**, 095001 (2007) [arXiv:0706.2997 [hep-ph]].
- [58] M. Misiak *et al.*, *Phys. Rev. Lett.* **98** (2007) 022002 [arXiv:hep-ph/0609232].
- [59] W. S. Hou, *Phys. Rev. D* **48** (1993) 2342.
- [60] A. Masiero, P. Paradisi and R. Petronzio, *Phys. Rev. D* **74** (2006) 011701 [arXiv:hep-ph/0511289].
- [61] Y. Miyazaki *et al.* [BELLE Collaboration], *Phys. Lett. B* **648** (2007) 341 [arXiv:hep-ex/0703009].
- [62] D. Black, T. Han, H. J. He and M. Sher, *Phys. Rev. D* **66** (2002) 053002 [arXiv:hep-ph/0206056].
- [63] M. Raidal *et al.*, *Eur. Phys. J. C* **57**, 13 (2008) [arXiv:0801.1826 [hep-ph]].
- [64] B. Aubert *et al.* [BABAR Collaboration], arXiv:0908.2381 [hep-ex].
- [65] K. Hayasaka *et al.* [Belle Collaboration], *Phys. Lett. B* **666** (2008) 16 [arXiv:0705.0650 [hep-ex]].
- [66] J. L. Diaz-Cruz, R. Noriega-Papaqui and A. Rosado, *Phys. Rev. D* **69**, 095002 (2004) [arXiv:hep-ph/0401194].
- [67] T. V. Kukhto, E. A. Kuraev, Z. K. Silagadze and A. Schiller, *Nucl. Phys. B* **371** (1992) 567.  
A. Czarnecki, B. Krause and W. J. Marciano, *Phys. Rev. D* **52** (1995) 2619 [arXiv:hep-ph/9506256].  
A. Czarnecki, B. Krause and W. J. Marciano, *Phys. Rev. Lett.* **76** (1996) 3267 [arXiv:hep-ph/9512369].

- [68] P. Paradisi, JHEP **0602** (2006) 050 [arXiv:hep-ph/0508054].
- [69] S. Nie and M. Sher, Phys. Rev. D **58** (1998) 097701 [arXiv:hep-ph/9805376].
- [70] R. A. Diaz, R. Martinez and J. A. Rodriguez, Phys. Rev. D **64** (2001) 033004 [arXiv:hep-ph/0103050].
- [71] S. K. Kang and K. Y. Lee, Phys. Lett. B **521**, 61 (2001) [arXiv:hep-ph/0103064].
- [72] V. M. Abazov *et al.* [D0 Collaboration], Phys. Rev. Lett. **102** (2009) 251801 [arXiv:0903.4800 [hep-ex]].  
CDF Collaboration, “ Search for Standard Model Higgs using tau leptons using  $2\text{ fb}^{-1}$ ”, CDF Conference Notes 9179.
- [73] D0 Collaboration, “Search for the SM Higgs boson in that tautauqq final state”, Conference Note 5845-CONF
- [74] D0 Collaboration, “Search for MSSM Higgs Boson Production in the Decay  $h$  to  $\tau_\mu \tau_{\text{had}}$ ”, Conference Note 5728-CONF
- [75] The TEVNPH Working Group, “Combined CDF and D0 upper limits on MSSM Higgs boson production in tau-tau final states with up to  $2.2\text{ fb}^{-1}$  of data”, FERMILAB-FN-0851-E, CDF Note 10099, D0 Note 6036-CONF.
- [76] S. Kanemura and K. Tsumura, Phys. Lett. B **674** (2009) 295 [arXiv:0901.3159 [hep-ph]].